MSc Thesis, 30 ECTS
ISRN LUTVDG / (TVTG-5137) / 1-62 /(2015)

Groundwater modelling of Färgaren 3 in Kristianstad

Simulations in MIKE SHE based on two extraction scenarios and different hydrogeological settings

Hanna Nordlander
Engineering Geology
Faculty of Engineering
Lund University

Thesis work for Master of Science 30 ECTS
Environmental Engineering

Groundwater modelling of Färgaren 3 in Kristianstad

Simulations in MIKE SHE based on two extraction scenarios and different hydrogeological settings

Grundvattenmodellering av kv. Färgaren i Kristianstad

Simuleringar i MIKE SHE baserade på två uttagsscenarier och olika hydrogeologiska förutsättningar

Hanna Nordlander
Engineering Geology
Faculty of Engineering
Lund University

Lund 2015

Supervisors:
Gerhard Barmen, Engineering Geology
Erik Mårtensson, DHI Sverige AB
Håkan Rosqvist, Tyréns AB
Charlotte Sparrenbom, Department of Geology

Examiner:
Jan-Erik Rosberg, Engineering Geology

Author:
Hanna Nordlander, 1987 –

Title:
Groundwater modelling of Färgaren 3 in Kristianstad - Simulations in MIKE SHE based on two extraction scenarios and different hydrogeological settings

Titel:
Grundvattenmodellering av kv. Färgaren i Kristianstad – Simuleringar i MIKE SHE baserade på två uttagsscenarier och olika hydrogeologiska förutsättningar

46 pages + 6 appendices (16 pages)
50 figures
9 tables

Acknowledgements

Special thanks to my main supervisor Gerhard Barmen at the Faculty of Engineering at Lund University for his support throughout the entire process of writing this thesis, and for his extensive and valuable feedback.

Warm thanks to my supervisors Charlotte Sparrenbom at Lund University, and Håkan Rosqvist at Tyréns AB, whom have both been very positive, motivating and inspiring during the time of my thesis. I would also like to thank my supervisor Erik Mårtensson at DHI Sverige AB for his patience, and for guiding me through the modelling in the, for me completely new, software MIKE SHE.

I would also like to extend my gratitude to DHI in Malmö for providing me with a license to the MIKE SHE software, and to Tyréns in Malmö for lending me a computer and offering me a desk to work at.

Moreover, I also want to thank C4Teknik at the municipality of Kristianstad for making this thesis possible by allowing me to work with their comprehensive groundwater model of the Kristianstad basin.

Last but not least, I thank Ted Kronvall for his never-ending loving support through my ups and downs.

Lund, February 2015

Hanna Nordlander

Abstract

This thesis aims to describe the hydrogeology and the groundwater flow variations in the area around Färgaren 3 in Kristianstad. The site was occupied by a dry-cleaning business between the years 1906 and 1988 and is now heavily contaminated with the chlorinated solvent perchloroethene (PCE). PCE, and some of its degradation products, are highly toxic. Spreading to the underlying sandstone aquifer, which is the largest groundwater resource in Sweden, could therefore have devastating effects.

A previously established regional groundwater model, in the modelling software MIKE SHE, forms the basis in this thesis. A sub-model, covering the area of interest is created, and is updated to attain a more detailed description of the local geology. Groundwater simulations are performed based on two different extraction scenarios, and using different versions of the updated groundwater model.

The results of the simulations show that the increased extractions from the sandstone aquifer during the twentieth century have had a major effect on the groundwater flow in the sub-model area. From being a discharge area, a large part of the area, including the contaminated site, is now a recharge area. Furthermore, the horizontal flow direction is altered. The flow is, due to the large extractions, directed to the municipal wells in central Kristianstad. To evaluate the potential spreading of PCE in this direction further studies, including contaminant transport calculations and groundwater samplings, are highly recommended.

Keywords: Groundwater modelling, MIKE SHE, perchloroethene (PCE), dry-cleaning business, contaminated soil, Kristianstad

Table of Contents

1. Introduction

Between the years 1906 and 1988 a dry-cleaning business operated at the site Färgaren 3 in the town of Kristianstad. The laundry buildings have been torn down, but large amounts of the solvent used in the dry-cleaning, namely perchloroethene (PCE), has contaminated the soil and the shallow groundwater in the area (Engdahl et al, 2011). PCE, and some of its degradation products, are carcinogenic (Guyton et al., 2014) and further spreading could potentially have devastating effects. The contaminated site is sitting on top of the largest groundwater aquifer in Sweden (C4 Teknik, 2000). A combination of the fact that PCE is harmful, together with the possible threat to a significant groundwater resource, places the site on a third place on the decontamination priority list in the county of Scania. This is just below BT Kemi in Teckomatorp and Klippan Läderfabrik (Länstyrelsen Skåne, 2013).

Many surveys have been undertaken in the area around Färgaren 3 to map the spreading of the contaminant, and to form a base for a decontamination of the site. A regional groundwater model, which covers the entire groundwater aquifer, already exists (C4 Teknik, 2000). The model has been used to simulate many different scenarios, investigating for example threats to the groundwater resource, and alternative extraction locations for drinking water. The model has been set up in the modelling tool MIKE SHE and will, together with extensive data from surveys, form the basis for this thesis.

Within the collaboration TRUST 2.1 research is conducted on contaminated sites (TRUST, 2015a). The focus in many of the projects is on chlorinated solvents and especially PCE. Several projects connected to the site Färgaren 3 has been carried out, whereof one aims to map the geology and the contamination using geo-electrical methods (resistivity and induced polarisation)(Lumetzberger, 2014). As a next step within TRUST 2.1, building on previous results, this master thesis aims to deepen the knowledge of the local groundwater movement and thus also improve the understanding of the transport of soluble contaminants in the area.

1.1 Aim

The overall aim of the master thesis is to:

- improve the understanding of the groundwater conditions around the site Färgaren 3 in Kristianstad. The focus will be on describing the hydrogeology in the area and the groundwater flow variations in time and space. As a secondary aim the transport of dissolved pollutants will be discussed.

The aim will be reached by:

- creating a sub-model within the established regional groundwater model.
- updating the geology within the sub-model based on recent field investigations.
- performing groundwater simulations based on two extraction scenarios and using different hydrogeological settings in the updated groundwater model.

1.2 Selection of modelling software

The established regional groundwater model, which forms the basis in this master thesis, is created in the software MIKE SHE. The same software is used in the simulations performed since it is considered problematic to transfer the model to another modelling software. MIKE SHE is regarded to be a highly advanced modelling tool, so the work on this thesis has had a rather steep learning curve.

1.3 Limitations

This thesis makes use of the detailed results from TRUST 2.1, and other technical surveys previously conducted in the area around Färgaren 3 by various consultant companies. No additional technical surveys are performed, and the local update of the regional groundwater model in MIKESHE is entirely based on the results from previous studies. Furthermore, the thesis does not include contaminant transport calculations. However, the spreading of dissolved PCE is briefly discussed based on the results from the groundwater simulations, and on the chemical and physical properties of the contaminant.

Another aspect limiting the comprehension of this study is time. As in many similar projects, the study could easily be expanded to include more simulations and covering additional simulation scenarios. To stay within the scope of the 30 ECTS of this MSc thesis, the study is limited to four different model versions and two extraction scenarios.

2. Background

2.1 Previous investigations

In addition to the established regional groundwater model (DHI and VBB Viak, 1998), documentation from recent investigations has been used in this study. As Färgaren 3 is ranked as the third most prioritised contaminated area in Scania, a great amount of data is available. Extensive field surveys have been carried out by consultant companies for the municipality of Kristianstad. These have formed the basis for a risk assessment performed by *Engdahl et al* (2011), which has provided essential background information to this study. The risk assessment, together with a related preparatory study (Engdahl et al, 2010), includes, e.g., numerous borehole logs, a conceptual model of the geology in the area (see Figure 4), a mapping of the contamination plumes (see section 2.6), and alternatives for a planned decontamination of the site.

Documentation from projects carried out within TRUST 2.1 has also had an important role in this study, and the results from *Lumetzberger* (2014) have been of special interest. The modelled resistivity profiles from Lumetzberger's electrical resistivity tomography (ERT) measurements contain valuable information on the geometry and characteristics of the geological units in the area. These are central in the updates of the geological models in this thesis.

2.2 TRUST – TRansparent Underground STructure

TRUST (TRansparent Underground STructure) is a research and development project in underground constructions, with the overall aim to promote research on sustainable development of urban underground infrastructure. The project is a collaboration between six different universities and specialists from the industry (TRUST, 2015b).

The TRUST project consists of nine sub-projects, all of which are working with the development of more efficient and sustainable methods, as well as tools, for planning, designing and constructing underground facilities (TRUST, 2015b). The sub-project TRUST 2.1 focuses on developing geoelectrical subsurface imaging techniques for use in urban areas. The ambition is to improve geophysical methods with regard to identifying geological features, groundwater, structures and pollution in urban environments (TRUST, 2015a). The field studies within TRUST 2.1 have so far mainly focused on the sites Färgaren 3 in Kristianstad, and Renen 13 in Varberg.

2.3 Site description and history

The site Färgaren 3 is located within the light industrial area Långebro in the town Kristianstad, located in the north-eastern part of Scania. The property has been vacant since the laundry buildings where demolished in 2001, and now the empty site is overgrown with grass, scrubs, and other undergrowth. Along the eastern side of the property there runs a bicycle path on an embankment. On the other side of the path there is a wetland area, extending to the river Helge å (see Figure 1). The Kristianstad city centre is located east of this river. Northwest of the site, just outside the figure, is a closed landfill located.

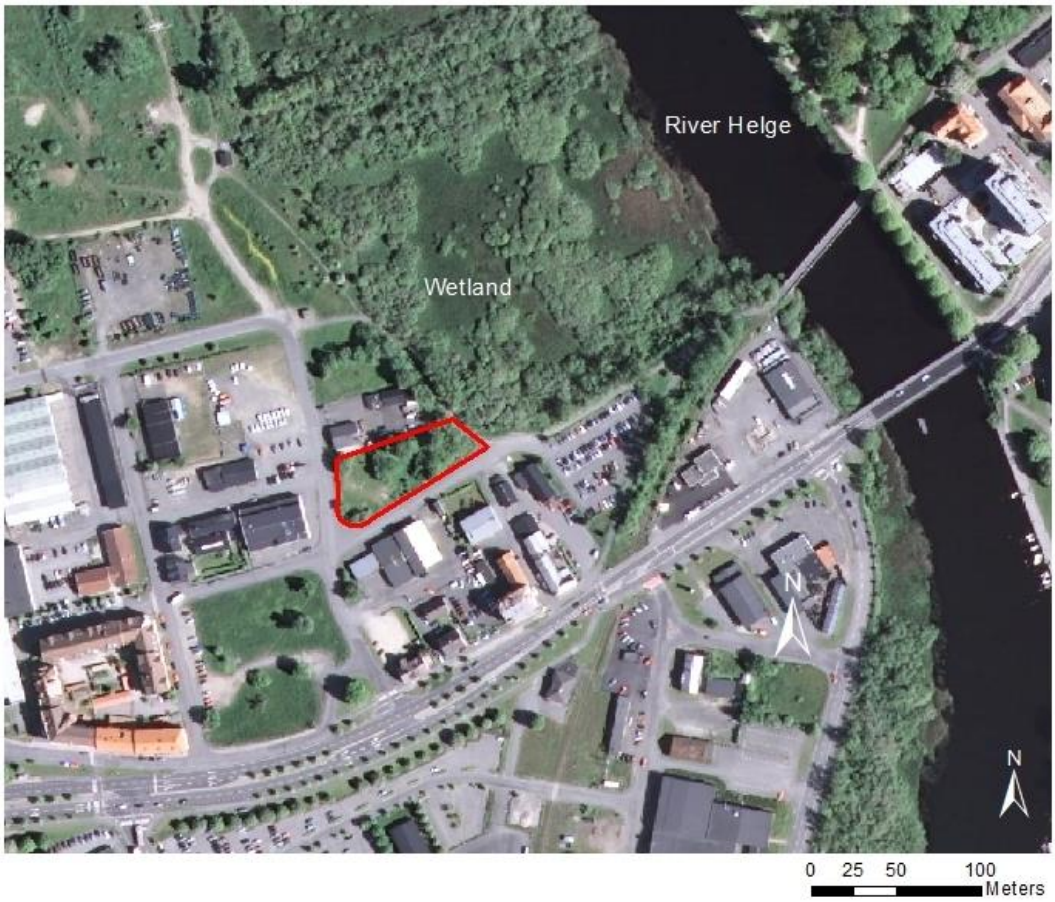

Figure 1. An overview of the area around the site Färgaren 3. The red polygon marks the location of the contaminated site and east of the site a wetland area can be found

In 1906 Anders Persson moved his dry cleaning business *Anders Perssons Färgeri och Kemtvätt* to the, at that time newly erected buildings at the address Färgaren 3. The business was run within the family until 1964 when it was assigned to Raoul Wangel. Wangel operated the business until 1988 when it closed. The laundry building was ultimately demolished in 2001 (Engdahl et al, 2011).

The facility was one of the first in Sweden to wash clothes using chemical solvents. During the time of operation the dry cleaner was equipped with at least one washing machine that used the solvent perochloroethene (PCE), which now can be found in great concentrations in the soil and the shallow groundwater in the area (Engdahl et al, 2011).

There is no existing documentation on where and how spent solvent was stored and handled, nor where it was disposed. Conducted interviews with former employees did not reveal any detailed information on where, or even if, spent solvent was poured out or buried within the premises during the period 1906-1964. However, former residents of Färgaren 3 relayed some information that suggested that waste might have been deposited in the swampy part of the premises east of the main building in the 1960s, near the wetlands marked in Figure 1 (Engdahl et al, 2011).

2.4 Regional hydrogeology of the plain Kristianstadsslätten

2.4.1 Regional geology

The plain Kristianstadsslätten rests upon a basin-shaped depression in the crystalline bedrock, filled with Cretaceous sedimentary bedrocks and Quaternary deposits. The basin is clearly limited by the horsts Nävlingeåsen and Linderöåsen in the southwest (see Figure 2), and less so in the north, levelling out gradually. The depth to the crystalline bedrock, mainly composed of gneiss and granite, varies greatly over the area and the total depth reaches more than 300 meters in the south. In some regions, the crystalline bedrock has suffered erosions, transforming it to quartz sand and kaolin, which is a type of clay (Gustafsson et al, 1979). Its presence and thickness varies greatly in the region.

The lower part of the Cretaceous bedrock consists of more or less consolidated glauconite sandstone. This layer is of particular interest from a hydrogeological viewpoint, as it holds the largest groundwater resource in Sweden (C4 Teknik, 2000). The aquifer is a confined porous aquifer, and its thickness is known to vary between 25 and 50 meters, around the city Kristianstad (Gustafsson et al, 1979).

On top of the sandstone rests an upper, and therefore later, Cretaceous bedrock layer, made up by different combinations of limestone, sandy limestone, and limy sandstone. These types of rock are distinguished by their respective ratios of lime to sand (Gustafsson et al, 1979). The distribution of this layer, in the horizontal plane, is defined in Figure 2.

The sedimentary bedrock is overlain by Quarternary deposits, which in general have a total thickness from 10 to 20 meters, and locally reaching a thickness of up to 50 meters. These deposits include till, glacial clay, glacio-fluvial deposits, shoreline deposits, and peat. Their respective horizontal distributions vary to a large extent over the area (Gustafsson et al, 1979).

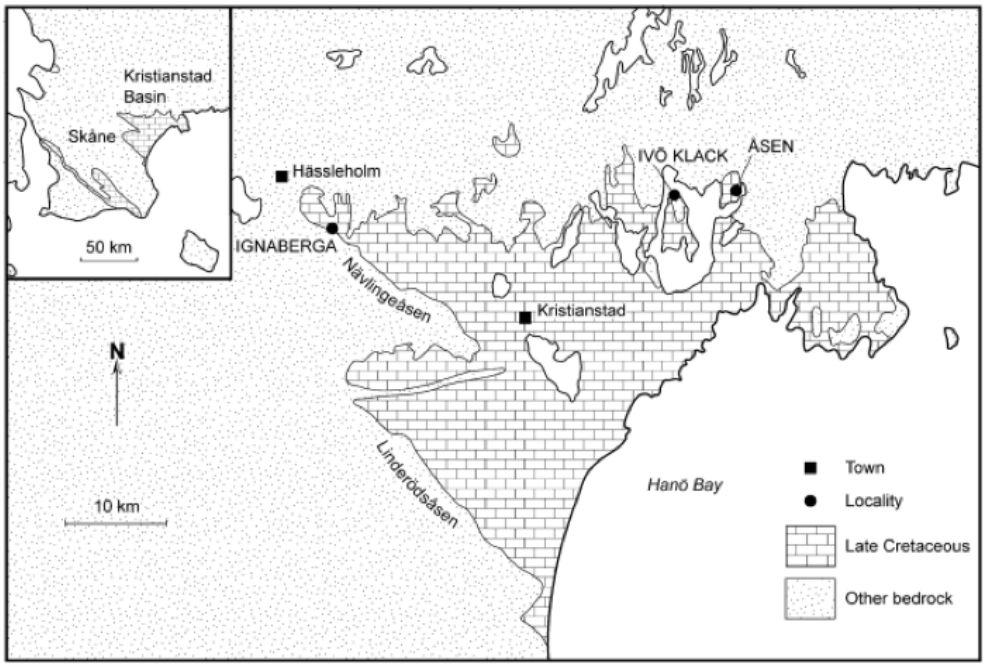

Figure 2. Map showing the location of the Kristianstad basin, and the distribution of the Later Cretaceous sedimentary layer within the basin. The basin is clearly limited by the horsts Linderöåsen and Nävlingeåsen in the southeast (Lindgren and Siverson, 2002, with permission from Lindgren)

2.4.2 Groundwater situation

The groundwater resource in the Kristianstad basin is exploited by many, and for many different purposes. About 3000-4000 drilled wells are found within the area of the basin, and the majority of these extract water from the lower sedimentary bedrock, i.e. the glauconite sandstone. The water is utilized for municipal water supply, irrigation, industrial purposes, geothermal heat exchangers, and individual households (C4Teknik, 2000). The estimated extracted volume per year, and number of drilled wells in each sector is presented in Table 1. The municipal wells and the irrigation wells dominate the extractions.

Table 1. Overview of the groundwater extractions from the sedimentary bedrock in the Kristianstad basin. The values are from C4Teknik (2000) and represent estimated values for the period 1980-1989. The extraction volumes are considered to be 5-10% greater today

Sector	Number of drilled wells	Extraction volume (Mm^3/year)
Municipal water supply	60-70	10.4 *
Agriculture	600-800	11.3
Industry	20-30	2.2**
Geothermal heating	100-200	1
Individual household	2000-3000	0.3

*whereof 4.6 in the town of Kristianstad, ** whereof 1.2 in the town of Kristianstad

In Kristianstad, the first drilled well was constructed 1939, and a couple of years later the entire water supply in the town was based on groundwater (C4Teknik, 2000). The municipal water consumption increased rapidly during the 1950's and the 1960's, and eventually become completely based on groundwater extractions (Gustafsson et al, 1979). As a response to the increasing demand, drilled wells were constructed at Näsby industrial area in 1947, and on the field Näsby fält north of the city in 1971 (C4Teknik, 2000).

The volumes of groundwater extracted for irrigation purposes increased substantially from the 1970's and onwards. The extractions are mainly focused on the summer months, i.e., May till August, and the volumes vary greatly between the years depending on the weather conditions (C4Teknik, 2000).

2.5 Hydrogeological conditions at Färgaren

2.5.1 Local geology

Information from the borehole logs in the preparatory study (Engdahl et al, 2010) has, together with previous measured geological data, been used to interpret the soil stratigraphy in the area around Färgaren 3 (Engdahl et al, 2011). The resulting geological model is presented in Figure 3 and in Figure 4.

The surface layer within the area is a highly heterogeneous fill material. The thickness of this layer varies from about half a meter to a maximum of 6 metres in the embankment towards the wetland. In the wetlands to the east, organic sediments (peat and dy) dominate the first ten meters. A thinner peat layer extends a few meters into the contaminated site. The layer underneath the fill and organic sediments is described as varved clay. The thickness varies a lot over the area and in some boreholes it is not observed at all. Within the eastern most part of the site the thickness of the clay increases distinctly, eventually reaching values of about 16 meters. Here, streaks of sand and peat are found within the clay, which has been interpreted as a historical shoreline, from a time when the river had a wider span (Engdahl et al, 2011). A layer

of till follows the clay layer. The content of the till is described as being dominated by silt and sand but coarse gravel, stones and at some locations even boulders are also present. Underlying the till, a formation of limestone is found. The exact position of the limestone is somewhat uncertain. It was difficult to extract an intact sample of the limestone and a boundary between the limestone and the till, which to a great extent consists of eroded limestone, has therefore been problematic to distinguish. The limestone formation overlies the glauconite sandstone and is approximately 75 meters thick. No fractured zones in the area around the contaminated site have been reported (Engdahl et al, 2011).

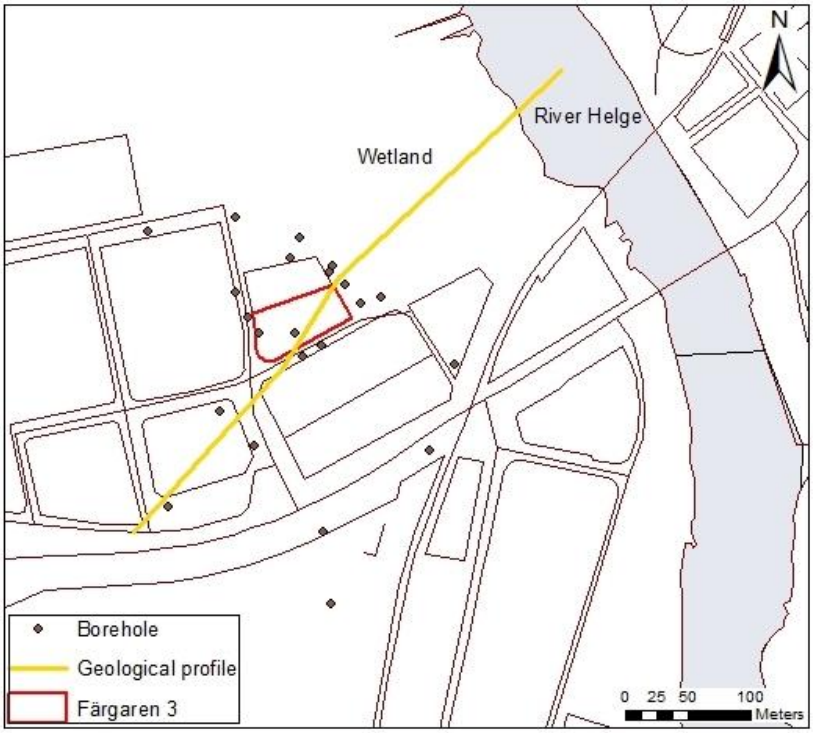

Figure 3. The location of geological profile in Figure 4 is presented as a yellow line in the figure. The boreholes from *Engdahl et al (2010)*, which are used in the update of the geological models, are also presented, and can be seen as brown dots

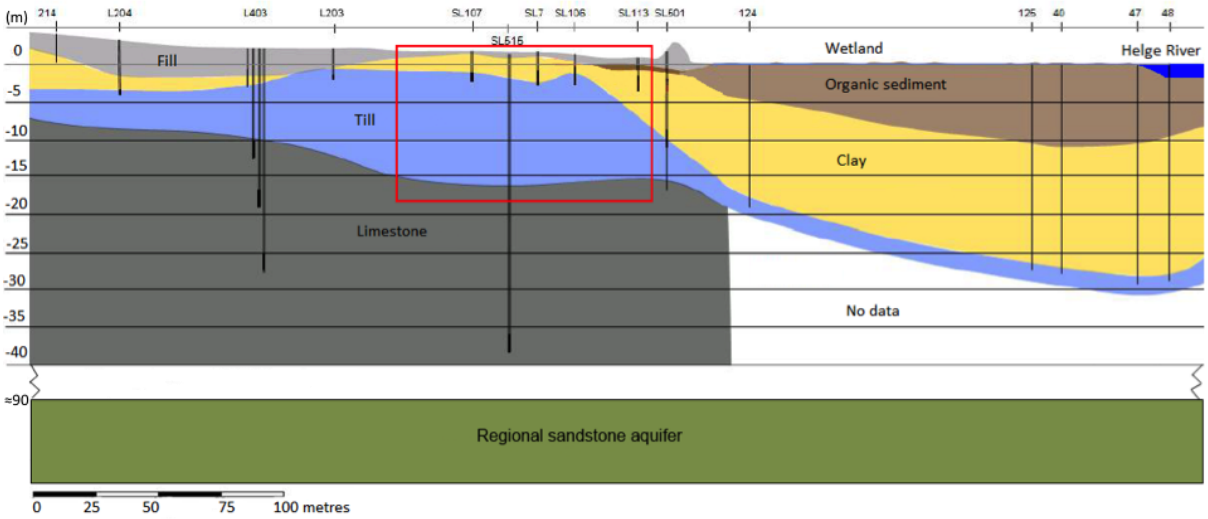

Figure 4. Geological model of the area around Färgaren 3. The red box marks the location of the contaminated site (Engdahl et al, 2010, with permission from Engdahl). The figure is modified, for all unmodified figures see Appendix A

Additional, and to this study significant, information on the geometry of the geology in the area is presented by *Lumetzberger* (2014). The information is based on ERT measurements and the locations of the performed measurements, as well as the modelled resistivity profiles are found in Figure 5, and in Figure 6 to Figure 11, respectively. Lumetzberger interprets the distinct resistivity boundary found in the profiles as the likely boundary between the layers of soil and the sedimentary bedrock. What is suspected to be an approximately 50-60 meters wide local depression in the bedrock is found under the west part of the contaminated site. The formation interpreted as the large depression can be seen in middle of line 20 and the most western part of line 2 and line 3. A depression at this location could potentially have a significant impact on the spread of contaminant in the area. The depth of the depression may however not be determined from the profiles. This could mean that the depression extends further down than the range of the profiles, although it should be noted that the uncertainty in the measured data increases with depth (Lumetzberger, 2014).

Similar depression with various depths can be seen in all resistivity profiles. The material in the depression is considered to be till with fractions of limestone. This may explain why the potential depressions have not been discovered in the extensive boreholes surveys, as the loose bedrock fragments might have been misinterpreted as bedrock surface (Lumetzberger, 2014).

Furthermore, Lumetzberger argues that the fill material, which generally has high resistivity, is relatively easy to distinguish in the profiles. See for example the high resistivity surface layer in Line 17 (Figure 6). The fill material distinguishes itself from the low resistant underlying layer, which is interpreted as clay. Not surprisingly, no fill is found in the eastern part of the profile, which extends out into the wetland. Read more about Lumetzberger's interpretations of the results and electrical resistivity tomography (ERT) measurements in *3-D and 2-D resistivity and IP mapping of geology and chlorinated aliphatics at Färgaren 3, Kristianstad* by *Lumetzberger* (2014).

2.5.2 Groundwater situation

The depth to the water table in the area is between 2 and 4 meters from ground level and it varies with the seasons. On average, this is one meter below the water level of the nearby river Helgeå, and also below sea level. The groundwater potential has been observed to decrease with increasing depth and the lowest levels are found in the sandstone. Furthermore, the vertical gradient between the till and the sandstone layer varies over time, although it was always directed downwards during the time of the survey. Thus, the contaminated site appears to be located within a recharge area (Engdahl et al, 2011).

The extractions from the porous sandstone aquifer in the area have a distinct influence on the groundwater at the contaminated site, even in the overlaying limestone and till. Groundwater level fluctuations that resembles the extraction pattern in the two industrial wells south of the contaminated site (see Figure 18) has been observed in a shallow well (9 meter deep) at Färgaren (Engdahl et al, 2011).

The horizontal hydraulic gradient in the lower levels of the till has also been measured. The direction varied over time during the survey, but the main two directions were to the east and to the southeast from the contaminated site (Engdahl et al, 2011).

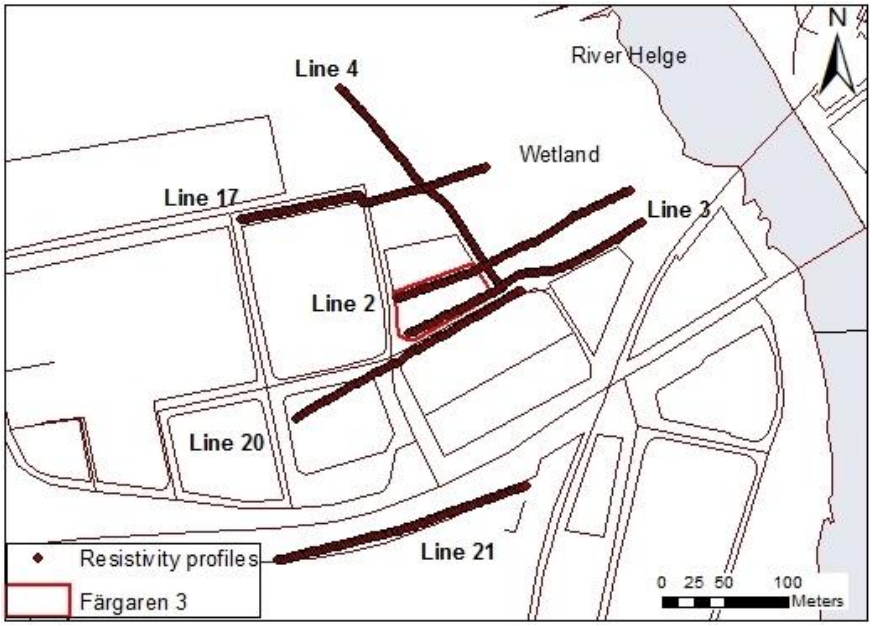

Figure 5. The locations of the ERT measurements performed by Lumetzberger (2014) are presented as dark red dotted lines in the figure. The modelled results of the measurements are found in Figure 6 to Figure 11

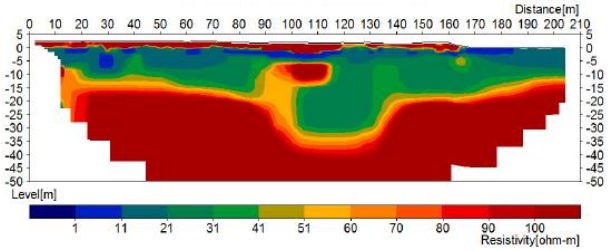

Figure 6. Resistivity profile line 17 (Lumetzberger, 2014, with permission from the author)

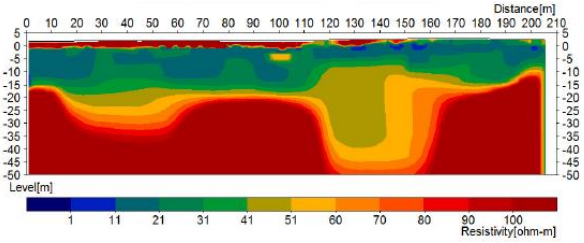

Figure 7. Resistivity profile line 4 (Lumetzberger, 2014, with permission from the author)

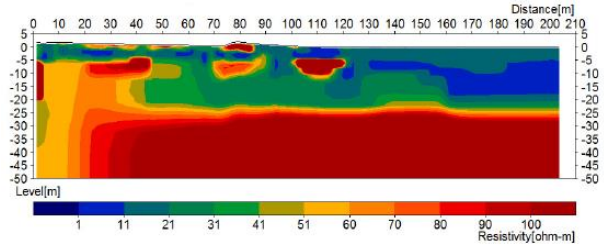

Figure 8. Resistivity profile line 2 (Lumetzberger, 2014, with permission from the author)

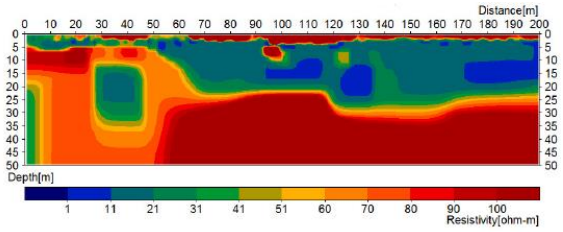

Figure 9. Resistivity profile line 3 (Lumetzberger, 2014, with permission from the author)

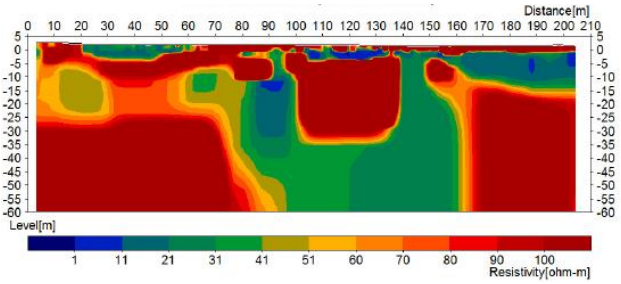

Figure 10. Resistivity profile line 20 (Lumetzberger, 2014, with permission from the author)

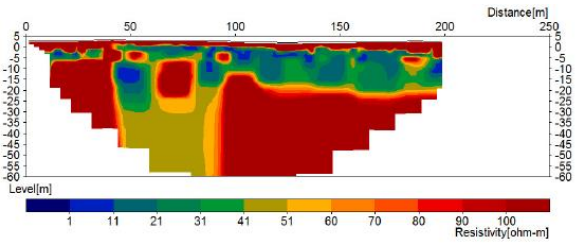

Figure 11. Resistivity profile line 21(Lumetzberger, 2014, with permission from the author)

2.6 Current contamination situation

The concentration of PCE in the soil within Färgaren 3 is extremely high, especially in the western part where the dry-clean facility was situated, and the property cannot be used at all before a complete decontamination has been performed. The contaminated soil acts as a long-term secondary source of pollution, which continuously contaminates the surrounding groundwater as the contaminant dissolves. The concentration of PCE in the groundwater in close contact to the contaminated soil and free phase PCE, reaches values to about a hundred thousand micrograms per litre, but decreases relatively fast with distance to approximately 1000 to 10 000 µg/L. The concentration in the fronts of the contamination plumes, around 200 meters from the source, is about 10 to 100 µg/L in PCE equivalents (Engdahl et al, 2011).

Figure 12 shows an interpretation of the contamination plume based on groundwater samples from both the till layer and upper part of the limestone. The plume can be seen to extend southwards, and eastwards, as well as to the northwest. The extensions to the south and to the east can be explained by the horizontal hydraulic gradients in the till which intermittently indicates groundwater flow in these directions due to large extractions. The dominating transport direction is today considered to be southwards, however it is possible that historically the main direction have been to the east, towards the municipal wells. The direction of transport is considered to be largely governed by the extractions, and is therefore likely to change if the extractions change. It remains unclear why traces of the contaminant are detected in groundwater samples northwest of the property, and it is suggested that they originate from a different source (Engdahl et al, 2011).

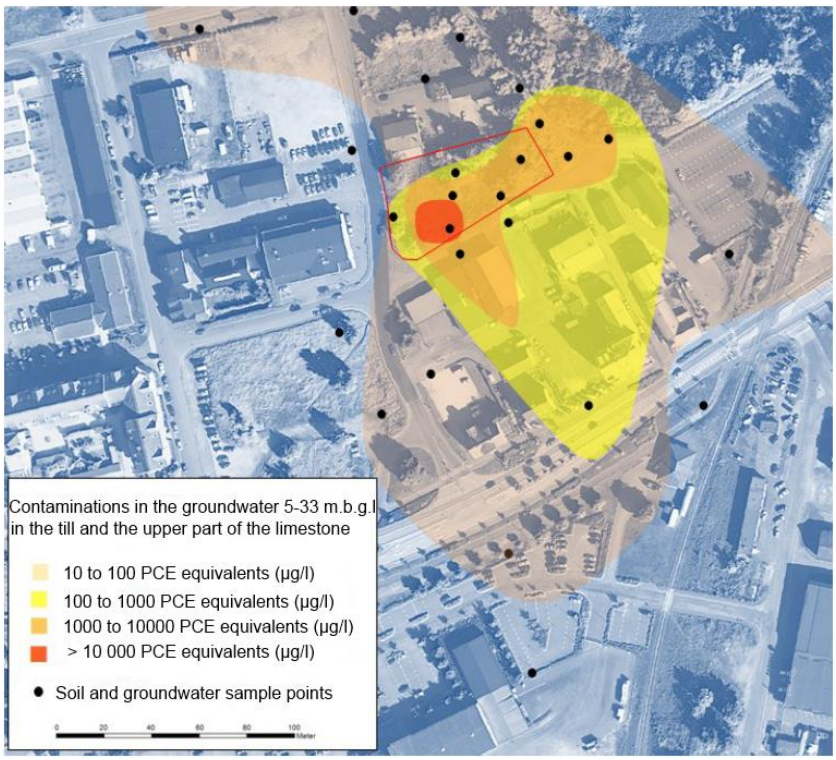

Figure 12. Interpreted extension of the contamination plume 5-33 meters below ground level based on groundwater samples in the area. The red polygon shows the location of Färgaren 3 and the groundwater sample points are marked with black dots (Engdahl et al, 2011, with permission from Engdahl). The figure is modified, for all unmodified figures see Appendix A

It has not been possible to limit the extension of the plume in the east since it has not been possible to make boreholes for groundwater sampling in the wetland. It is considered likely that the plume extends further and with higher concentrations in the till below the wetland than what may be seen from the figure (Engdahl et al, 2011).

The horizontal distribution of the contaminant increases with depth within the soil layers and the plume is larger in the till than in the overlying, less permeable, layers. The results of the groundwater samples also indicate that the contaminated groundwater has reached the top most part of the limestone (about 30 meters below ground level) but not further down (Engdahl et al, 2011).

2.7 Decontamination and future plans

To allow any future usage of the property and to reduce the threat to the groundwater aquifer, decontamination of the soil and shallow groundwater at Färgaren 3 is planned (Kristianstad kommun, 2015). The most common procedure in Sweden is to excavate the contaminated soil and then to transport it away to treat it elsewhere (Nordin, 2014). At Färgaren, a to Sweden new in-situ thermal remediation is planned.

The decontamination will be focused on the most heavily contaminated areas within the property. The top most layer of the contaminated soil (0-2.5 meters) will be removed and replaced with clean soil. In a next step, the more deeply located contaminants (2.5-20 meters) will be removed by heating up the soil and groundwater using either Electric Resistance Heating (ERH) or Thermal Conductive Heating (TCH). The contaminant and groundwater will then evaporate and the steam is collected at the surface. Once at the surface, the steam condensates to water and the remaining contaminated vapour is cleaned using activated carbon filters (Bank, 2014).
No decontamination of the contaminated groundwater outside the thermally treated area is planned. The spreading of the contaminant will be supervised and is expected to reduce through natural reductive dechlorination, i.e., through biological degradation. The degradation process will however be stimulated by injection of a carbon source if the concentrations have not reached desired levels after five years (Bank, 2014).

Kristianstad municipality is applying for a governmental grant at Naturvårdsverket to cover the decontamination cost. If the application is approved, the decontamination is scheduled to start in the spring of 2016 (Kristianstad kommun, 2015).

3. Theory

The theory chapter gives an overview of some important properties of the contaminant perchloroethene (PCE) and its degradation products. A short introduction to numerical groundwater modelling is also included.

3.1 Perchloroethene (PCE)

The chlorinated aliphatic hydrocarbon perchloroethene (PCE), also known as tetrachloroethene, is widely used within the dry cleaning business. Like other chlorinated solvent PCE is an excellent solvent for hydrophobic substances and has low solubility in water (Kemikalieinspektionen, 2015). Chlorinated solvents are also denser than water and are often referred to as Dense Nonaqueous Phase Liquids (DNPLs). These properties influence the way PCE spread in the soil and groundwater. PCE is initially transported vertically through the ground as a free phase, leaving behind disconnected blobs and strings, until it reaches a dense geological layer (Englöv et al, 2007). Since PCE is only slightly soluble in water, accumulated contaminant can persist for several decades or even hundreds of years (Kueper et al, 2003). Further transport occurs when PCE is slowly dissolved by the passing groundwater, generating aqueous phase plumes of contaminant. The groundwater flow governs the spreading of the dissolved contaminant and the contaminant plumes are gradually diluted through dispersion and natural degradation (Englöv et al, 2007). PCE is naturally degraded through microbial reductive dechlorination in sub-surface anaerobic conditions (see Figure 13). The degradation activity varies greatly from site to site, and the rate decreases with each degradation step (Vogel et al, 1987).

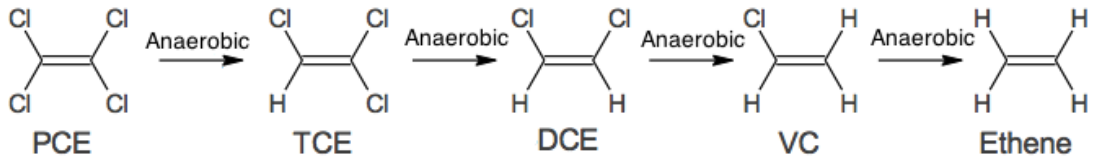

Figure 13. The natural PCE degradation process in anaerobic conditions. Modified from Wiegert 2013

The physical and chemical properties of PCE and its degradation products are presented in Table 2. Note that the density and the soil organic carbon-water partitioning coefficient (K_{oc}) decrease with each degradation step, whereas the solubility increases. The K_{oc} value describes the ratio of contaminant sorbed to the organic carbon in the soil to the concentration of the contaminant in the water. A low K_{oc} value is characteristic of a weakly sorbed compound, which is not significantly retarded relative to the rate of the groundwater flow (Kueper et al, 2003).

Table 2. The physical and chemical properties of PCE and its degradation products. All data is from RAIS (2015) and the chemical profile for the respective compound

	PCE	**TCE**	**DCE**	**VC**
Name	Tetrachloroethene (Perchloroethene)	Trichloroethene	Dichloroethene	Vinyl Chloride
Formula	C_2Cl_4	$C_2H_1Cl_3$	$C_2H_2Cl_2$	C_2H_3Cl
Molecular weight (g/mol)	165,8	131,4	96,9	62,5
Density (g/mL)*	1,62	1,46	1,28 (1,28)	0,91
Boiling point (C°)	121	87	55	-13
Solubility (g/L)**	0,2	1,3	3,5	2,8
Partition coefficient Koc (L/kg)	251	100	36	19

*at 20 C°, ** at 25 C°

The guideline values for drinking water quality and the cancer classifications of PCE and the degradation products are presented in Table 3. Note that VC is the compound that is placed in cancer classification group 1, and has the lowest limit value for drinking water quality.

Table 3. The cancer classification (IARC, 2015) and guideline values for drinking water quality (WHO 2011) for PCE, TCE, DCE and VC. The classification groups means: 1 - carcinogenic to humans, 2A – probably carcinogenic to humans, 2B – Possibly carcinogenic to humans, 3 - Not classifiable as to its carcinogenicity to humans

	PCE	**TCE**	**DCE**	**VC**
Cancer classification group	2A	2A	3	1
Guideline value for drinking water (µg/L)	40	20	50	0,3

3.2 Numerical groundwater modelling

The groundwater movement in a mathematical groundwater model is described by the solutions to equations of groundwater flow. The most basic of these equations is the empirically derived Darcy's law, which describes flow as a function of hydraulic conductivity and difference in hydraulic head. Darcy's law is presented in Equation 1:

$$Q = -KA\frac{\partial \phi}{\partial L} \quad , \qquad \text{(Equation 1.)}$$

where Q, A, K, $d\phi/dL$ denotes groundwater flow, cross-section area where flow passes, hydraulic conductivity, and hydraulic gradient. This equation is stated in one dimension, and is limited to a one-dimensional flow of a homogeneous incompressible fluid. However, the same relationship holds just the same in three dimensions and may be generalised as presented in Equation 2:

$$\boldsymbol{q} = -K\ grad\ \phi\ , \qquad \text{(Equation 2.)}$$

where $\boldsymbol{q}$ and $-\ grad\ \phi$ denotes a vector with the components q_x, q_y and q_z, and the hydraulic gradient with components $-\frac{\partial \phi}{\partial x}$, $-\frac{\partial \phi}{\partial y}$ and $-\frac{\partial \phi}{\partial z}$, in the xyz directions, respectively. The equation may be further developed and specified for flow through various types of aquifers, and for homogeneous compressible fluids (Bear and Verruijt, 1987).

Equation 2 contains two dependent variables, i.e. q(x,y,z,t) and ϕ(x,y,z,t), and to obtain a complete description of the flow in a given aquifer one additional equation is required. This

equation is based on the basic law of mass conservation and by solving it, using appropriate boundary and initial conditions, the distribution of $\phi = \phi(x,y,z,t)$ in a specified aquifer may be obtained. For a nonhomogeneous and anisotropic aquifer the mass balance equation may be defined as presented in Equation 3:

$$\frac{\partial}{\partial x}\left(K_x \frac{\partial \phi}{\partial x}\right) + \frac{\partial}{\partial y}\left(K_y \frac{\partial \phi}{\partial y}\right) + \frac{\partial}{\partial z}\left(K_z \frac{\partial \phi}{\partial z}\right) = S_0 \frac{\partial \phi}{\partial t} \ , \qquad \text{(Equation 3.)}$$

where S_0 is specific storativity (Bear and Verruijt, 1987).

If the equation parameters may be assumed to be constant in the aquifer, and the aquifer boundaries are relatively simple, the governing equations will reduce in complexity and may be solved analytically. If instead the boundaries are complicated, and the different model parameters vary throughout the aquifer due to heterogeneity and/or anisotropicity, the groundwater flow will follow a set of partial differential equations (PDE), which often must be solved numerically (Fetter, 2014).

Numerical models provide approximate solutions to the model equations by a discretization of both time and space. At each discrete point, the differentials in the PDEs are replaced by finite differences. For example, the hydraulic gradient, at each of these points, is approximated by a modeled difference in hydraulic head. The two main methods for finding these numerical solutions are the Finite Element Method (FEM) and the Finite Difference Method (FDM) (Igboakwe and Achi, 2011). In FDM, the spatial dimensions are discretized into a rectangular grid, in which the set of values that solve the model equations are piece-wise constant. This means that for each of the rectangles that make up the grid, the solution to the model equations is constant. In FEM, the spatial dimensions are instead divided into polygonal cells, which are typically triangular. Rather than constant, the solution in each cell is the result of an interpolation between grid points, which are placed in the corners of the polygon. As a result, the FEM solution is much smoother than FDM (Fetter, 2014).

For a more thorough description of the theory of groundwater flow and numerical modelling see *Bear and Verruijt* (1987) and *Fetter* (2014).

4. Method and material

4.1 MIKE SHE

The modelling and simulation software MIKE SHE may be used for simulations of all processes connected to the ground and surface water within a given catchment area. The entire land phase of the hydrological cycle can be simulated using established equations and physical data. Figure 14 shows a principal sketch of the modelling tool and its six main components: snow melt, interception and evapotranspiration, overland and channel flow, unsaturated flow, groundwater flow (saturated flow) and exchange between aquifers and surface waters (DHI and VBB Viak, 1998).

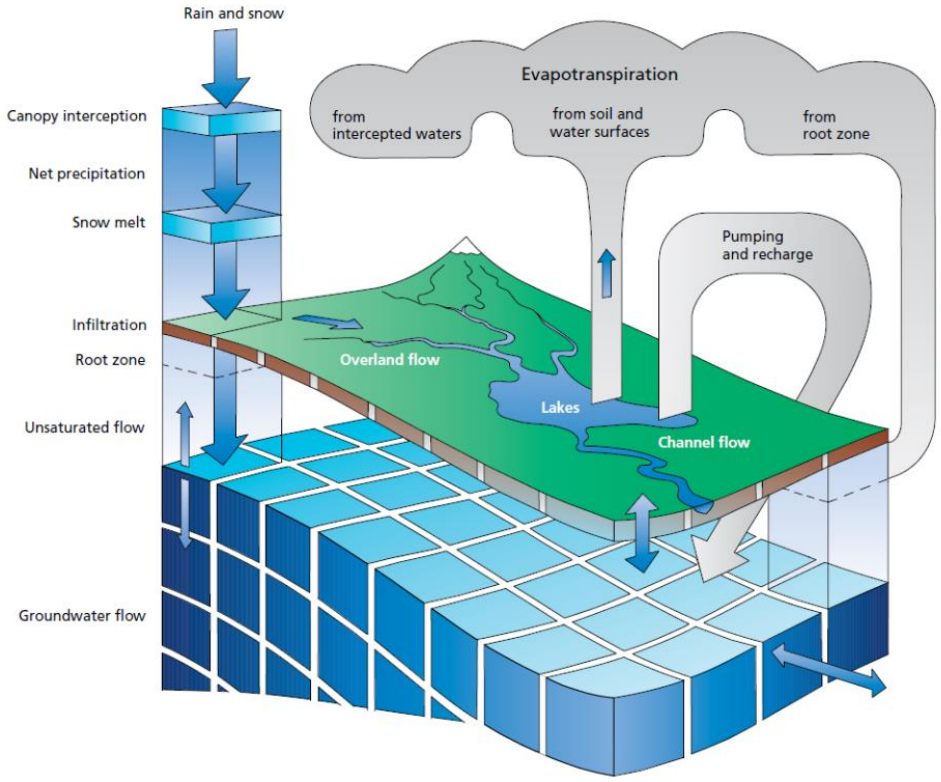

Figure 14. Principal sketch of the modelling tool MIKE SHE. The six main components are snow melt, interception and evapotranspiration, overland and channel flow, unsaturated flow and groundwater flow and exchange between aquifers and surface waters (DHI, 2014)

MIKE SHE gives a detailed description of the hydraulic and hydrological processes but, as a consequence, large amount of input data is required (C4 Teknik, 2000). The software is described as a distributed and physically based model, meaning that generally all data is of physical nature and geographically distributed (spatial data) within the catchment (DHI and VBB Viak 1998). The input can be constant (e.g. topography and hydraulic conductivity) or vary over time (precipitation and temperature).

The modelled catchment area is discretized onto a 2D square grid with a set resolution. The grid is used in both the overland flow and groundwater flow component. The two components are connected by a vertical column of nodes at each grid point representing a one dimensional (vertical) flow in the unsaturated zone. The water movement in the catchment is modelled by a numerical solution (finite difference based) of the partial differential equations describing the water flow within, and between the components of the model (DHI and VBB Viak, 1998).

A more detailed description of the MIKE SHE software is found in *MIKE SHE –User Manual* (DHI Software 2014).

4.2 Established regional groundwater model

In 1995, the municipality of Kristianstad initiated a survey with the goals of mapping the potential threats to the groundwater supply in Kristianstad, as well as evaluating future possible locations for new groundwater wells in the area. This survey was primarily based on results from previous geological and hydrogeological investigations. Its main contribution was that the entire data collection was processed using the modelling tool MIKE SHE, enabling a more holistic view for thorough analysis (C4 Teknik, 2000).

The survey resulted in a hydrogeological model, which comprehends all surface and groundwater in the plain Kristianstadsslätten, as well as the flows in and out of this area. The model took three years to establish and was developed in collaboration between C4-teknik, DHI, VBB Viak (later Sweco) and SGU. After the model was completed in 1998, it has been updated twice, during 2004 and 2010 (read more about the update in DHI 2005 and DHI 2011).

4.2.1. Model area and boundaries of the regional model

The groundwater model covers the plain Kristianstadslätten, the peninsula Listerlandet, and adjacent catchments (see Figure 15). Exceptions are the catchments of the rivers Helgeå and Skräbeå upstream Torsebro and Näsum, respectively, which are excluded to limit the size of the model and thus ensuring high numerical precision. To compensate, measured flows from these catchments are set as boundary conditions.

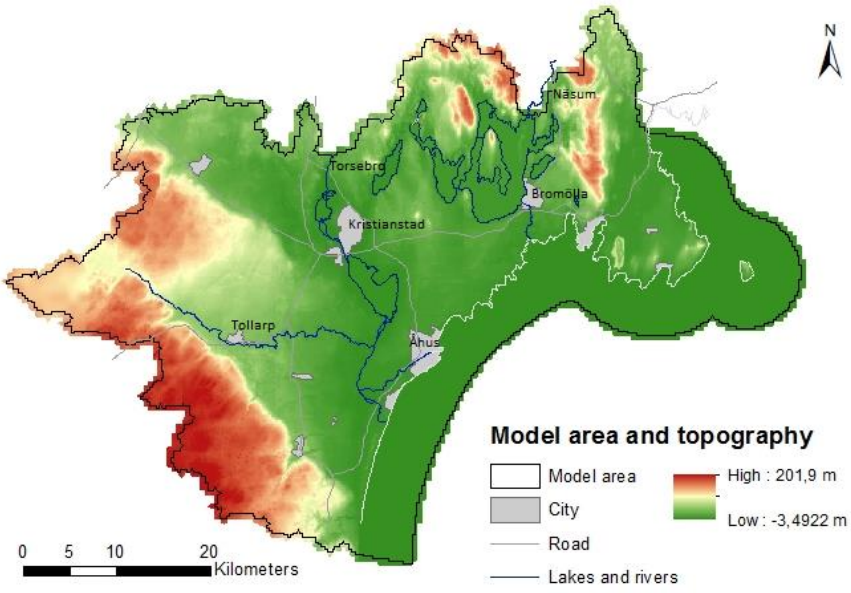

Figure 15. The model area and the topography of the MIKE SHE model. The model boundary in the east is set 5 km out into the sea and the total model area is 2350 km²

The boundary of the model area has been drawn using the contour lines on the 1:50 000 topographic map from Lantmäteriet to coincide with the boundary of the catchment. This corresponds to the topographic water divide and simplifies the setting of the boundary condition (no flow boundary). In the east the boundary is drawn 5 km from the coast and the boundary is set to a groundwater potential of 0 meter (normal sea level). The total model area is of 2350 km^2 (DHI and VBB Viak, 1998).

4.2.2. Overview of geometry and properties of the regional model

The geology of the area that the model covers is complex and consists of many diverse layers of soil and bedrock. In the model, the geology has to be simplified and layers with similar structure and hydraulic properties are therefore merged into larger layer units, with consistent relative order. This has resulted in a total of five layers of soil, referred to as peat, sand, clay, gravel and till, followed by the sedimentary bedrock of limestone, sandstone and finally the crystalline bedrock (DHI and VBB Viak, 1998). The composition of these layer units is presented in Table 4.

Table 4. The composition of the geological layer units in the regional model (modified from DHI and VBB Viak, 1998)

Layer unit	Soil and bedrock types
Peat	Postglacial peat, dy, clay, silt and sand (deposits form rivers, fens, lakes and the sea)
Sand	Postglacial sand and gravel (shoreline deposits)
Clay	Glacial and postglacial clay and silt
Gravel	Glacial sand and gravel (glaciofluvial deposits)
Till	Sandy - clayey till and boulder clay
Limestone	Cretaceous limestone, chalk limestone and sand limestone
Sandstone	Cretaceous glauconite sandstone
Crystalline bedrock	Precambrian crystalline gneiss and granite

Within the MIKE SHE-model there is a difference between the simplified geological model and the numerical model. The geological model consists of the eight geological layers defined above. A number of hydrogeological parameters (hydraulic conductivity, specific yield, and specific storage) are defined for each geological layer and the values vary spatially over the area of the model. The numerical model of the saturated zone instead consists of five computational layers, corresponding to one or more of the geological layers in the geological model (see

Figure 16). The fifth computational layer, corresponding to the crystalline bedrock, is not included in the figure. The hydraulic parameters of the computational layers are calculated as weighted means, using the parameters defined in the geological layers, where the weight is determined by the thickness of each layer (DHI and VBB Viak, 1998).
For more detailed description of the regional groundwater model of the plain Kristianstadsslätten see *Dokumentation av MIKE SHE-modellen för Kristianstadsslätten* by *DHI and VBB Viak* (1998), and the documentation of the two updates presented in *DHI* (2005) and *DHI* (2011).

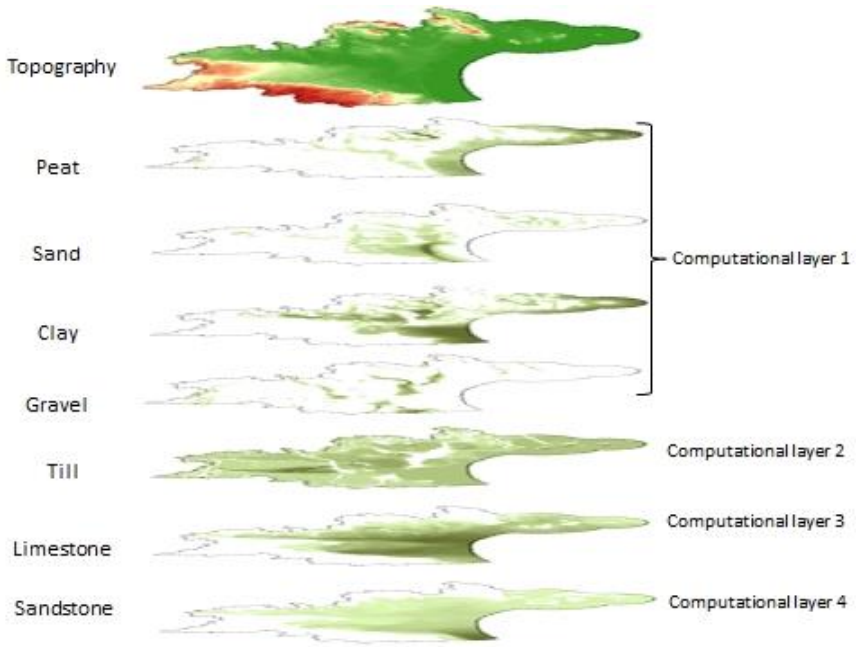

Figure 16. The geological layers included in the geological model and the corresponding computational layers in the numerical model. The sandstone layer rests on the crystalline bedrock, which corresponds to computational layer 5 (not included in the figure)

4.3 Model application

The regional groundwater model for the basin of Kristianstad may be, and have been, used to simulate many different scenarios for various purposes. For areas of special interest, sub-models can be created within the model, using results from the entire model as boundary conditions (Gustafsson et al., 1997).

In this study, a sub-model covering an area of 40 km^2 is created for the contaminated site (see Figure 17 and Figure 18). The grid size for this model is converted to 25 by 25 meters from the original 100 by 100 meters, allowing a detailed update of the geology in the area around Färgaren 3. The dotted line in Figure 18 shows the local area in which the geology is updated. The simulation results from the regional model are set as boundary conditions for the sub-model.

The sub-model area includes large parts of Kristianstad city. All extraction wells, which today contribute to the water supply of the city, are found within the boundaries of the sub-model, as well as many groundwater wells for industrial purposes. Note the two industrial wells south of Färgaren and the line of municipal wells at the east side of the River Helgeå, all which most likely will have a significant impact on the groundwater movement at Färgaren (see Figure 18).

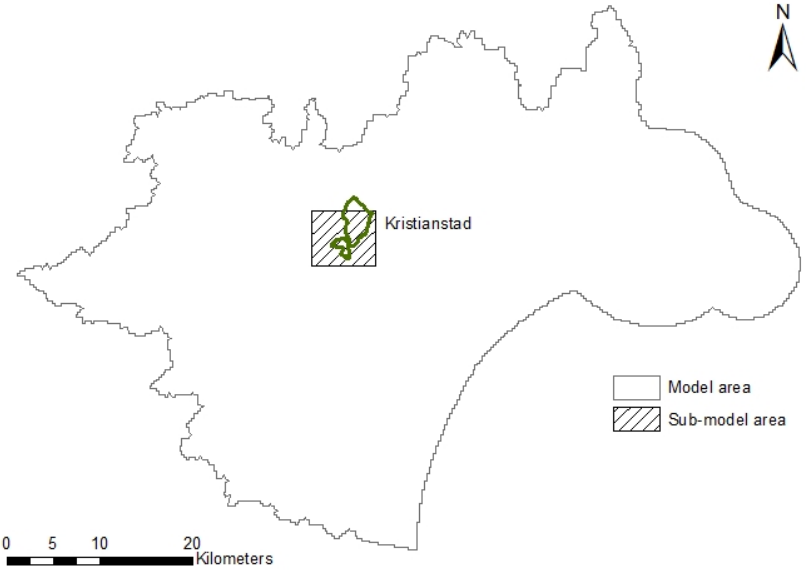

Figure 17. The position of the generated sub-model within the original model area. The green polygon represent the town of Kristianstad

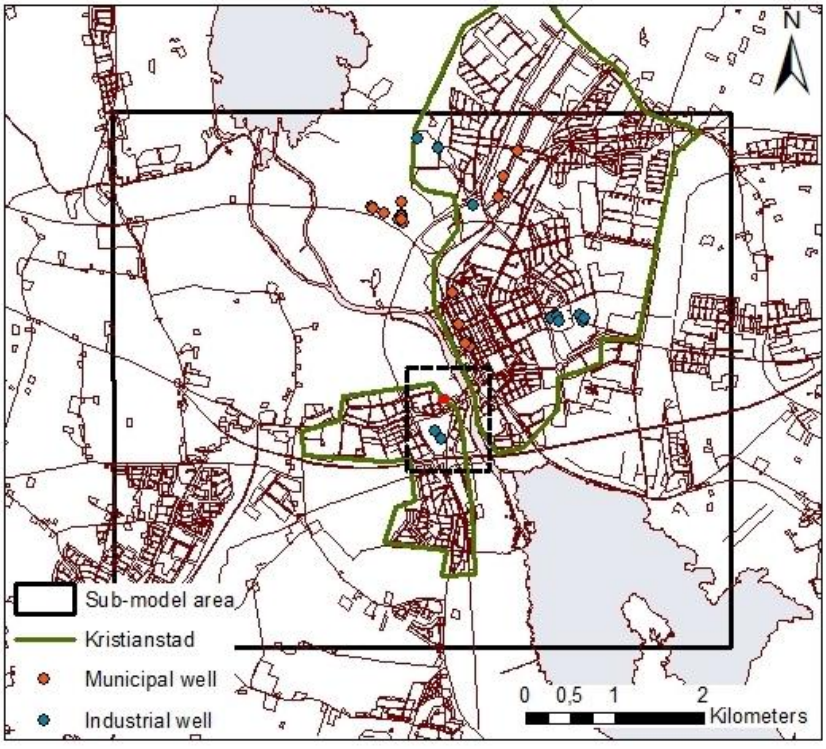

Figure 18. Close up of the sub-model area. The sub-model covers larger parts of Kristanstad city. The dotted line marks the area in which the geology is updated and the contaminated site Färgaren 3 can be seen as a red polygon in the centre of the figure

4.4 Groundwater simulations

The simulations performed in this study are based on two different groundwater extraction situations. The first extraction situation, from now on referred to as scenario A, represents the conditions in the early twentieth century when no significant amount of water was extracted from the groundwater aquifer of the plain Kristianstadsslätten. The second extraction situation, scenario B, represents the extraction situation of today when large volumes of water are extracted from the same groundwater aquifer. In scenario B, the municipal and industrial extractions are based on reported data from 2010. The extractions for irrigation purposes derive from estimations which were done when the MIKE SHE model first was established.

Four different geological models, referred to, as 0, 1, 2 and 3, will be used in the simulations in this study. Geological model 0 is an unchanged version with geology from the regional model, and model 1, 2 and 3 are updated versions using detailed information from recent studies. Model 1 is based on the borehole logs and geological profile from *Engdahl et al* (2011) (see Figure 3 and Figure 4) whilst model 2 and 3 also include additional information acquired from Lumetzberger's resistivity profiles (see Figure 5 and Figure 6-11). The extraction scenarios and versions of geological models are summarized in Table 5.

Table 5. Summary of the groundwater extraction scenarios and geological models used in the simulations

Groundwater extraction scenarios	
A	Early 20th century – relatively undisturbed conditions in the aquifer, minor extractions
B	Present day – large volumes of water extracted from the aquifer
Geological models	
0	Unchanged – geology from the regional model
1	Geology updated based on boreholes
2	Geology updated based on boreholes and resistivity lines
3	Alternative update of the geology based on boreholes and resistivity lines

The following combinations of the extraction scenarios and geological models are run: 0A, 0B, 1B, 2B, and 3B. In all simulations, the same set of measured climate data is used as input. Read about how and when the input data was measured in *DHI and VBB Viak* (1998), *DHI* (2005) and *DHI* (2011). Ten years of transient simulations are performed and the results are analysed according to the flow chart presented in Figure 19.

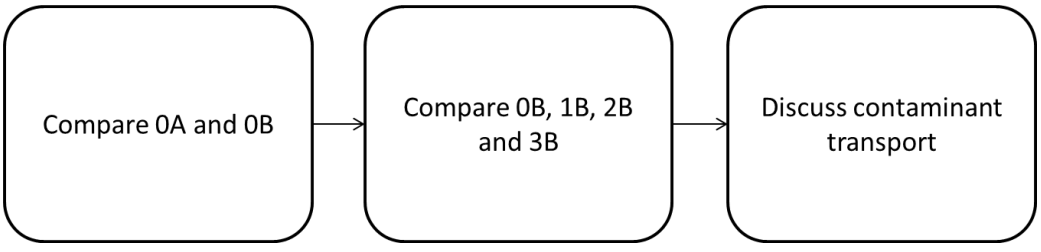

Figure 19. Flow chart describing the structure of the analysis of the results

As a first step, the result from the simulations of the unchanged model 0 for the two extractions scenarios A and B are compared. This creates an opportunity to analyse how the groundwater flow has changed in the area over time as a consequence of the extractions from the sandstone. In the next step, the simulation results from the three updated geological models are compared. This step will serve as a sensitivity analysis, forming the basis of a discussion about the

importance of detailed knowledge of the hydrogeology in the area. Finally, the last step includes a discussion regarding the transport of the contaminant, or rather the more soluble degradation products. The discussion will be based on the analysis of step 1 and 2, as well as on results from previous surveys and relevant theory.

4.5 Method for updating the geological model

The new updated versions of the geological model are created with an ambition of producing a more accurate and detailed description of the geology within the sub-model. The update is limited to the area around Färgaren 3, where the extended surveys have been focused (see marked area in Figure 18). Furthermore, the depth of the boreholes limits the update not further down than to the top of the limestone. Within the area of the update, this leaves a total of three geological layers to be updated: peat, clay and till. Furthermore, an additional layer of fill material, not included in the original model, is created. As a first step in the update, conceptual models for each of the three model versions are created.

The conceptual models consist of horizontal overviews of each separate geological layer. Not all interpretations of the geological layers are unique within the three model versions, e.g. the interpretation of the peat layer and the clay layer are the same for all three versions since no additional information where retrieved from the resistivity profiles. The main difference between geological model 1 and 2 is the introduction of the potential depression that was discovered in Lumetzberger's results. The geological model 3 is an alternative version of geological model 2 and the only difference between the two are the hydraulic conductive of the material in the depression. The properties of the depression is defined in the till layer, hence the difference between the models is found there. For an overview of these model differences, see Table 6.

Table 6. Overview of the differences between the updated models. All versions of the geological layers within each model are not unique, and the table illustrates the combination of layer versions in the different models. The abbrevations stands for fill version (FV), peat version (PV), clay version (CV), and till version (TV)

Model	Fill	Peat	Clay	Till
0	[none]	[unchanged]	[unchanged]	[unchanged]
1	FV-I	PV-I	CV-I	TV-I
2	FV-II	PV-I	CV-I	TV-II
3	FV-II	PV-I	CV-I	TV-III

As a next step, the conceptual models are digitalised in the modelling software MIKE SHE, and then incorporated into three new versions of the numerical model. Profiles from the resulting numerical geological models are presented in section 5.1. When possible, the hydraulic parameters from the unchanged model are used. This way the focus is kept on refining the geometry of the geology, preventing the risk of introducing too many variables into the analysis of the results. The hydraulic parameters of the unchanged model are presented in Table 7.

Table 7. The hydraulic parameters of the geological units in the original model. These are horizontal hydraulic conductivity (K_H), vertical hydraulic conductivity (K_V), specific yield (S_y) and specific storage (S_s)

Geological unit	K_H (m/s)	K_V (m/s)	S_y	S_s (1/m)
Peat	$1 \cdot 10^{-8}$	$1 \cdot 10^{-9}$	0.01	0.001
Clay	$1 \cdot 10^{-8}$	$2 \cdot 10^{-9}$	0.01	0.001
Till	$1 \cdot 10^{-6}$	$2.5 \cdot 10^{-7}$	0.05	0.001

The first step in digitalising the conceptual models is to convert the existing grid layers describing the layer thickness of each geological layer to the new resolution of 25 meters. The values within the area to be updated is then deleted, whereafter points or lines of known layer thickness are inserted. Next, some trial-and-errors are done, interpolating values onto the entire grid, using inverse distance weighting. In this process, the interpolation parameters are varied until a satisfactory thickness distribution of each layer is obtained. This should resemble the overview of each geological layer as much as possible. In the process some compromises between the conceptual model and the established model had to be done, as to create a smooth conversion between the updated area and the values of the original model. The fill material, commonly found as a top layer in urban areas are not included in the established regional model and a completely new grid layer had to be created. Otherwise, the same procedure as for the other layers was followed.

In the next subsections follows a description of the interpretation of geological layers and the assumptions made when creating the conceptual models. All horizontal overviews are found in Appendix F together with the unchanged version and the digitalised version of each layer (see **Figure 36** to Figure 50). The overviews include the boreholes (location and observed thickness), which they are based on, as well as the locations of the resistivity lines.

4.5.1 Fill layer

Assumptions regarding the distribution of fill material cannot be based on the same reasoning as when it comes to the naturally formed geological layers, where support can be found in underlying formation processes. Besides the observed values, the interpretation of the distribution of the fill material is based on its intended purpose, and derives from engineering reasons rather than geological processes. It is assumed that there is no fill on unexploited land, such as the wetland east of the contaminated site. From the borehole logs in *Engdahl et al* (2010), it was determined that the greatest known thickness of fill material is found in the embankment towards the wetland along the east side of the property. Furthermore, the thickness of the fill appears to vary between 1.5 and 3.5 meters in developed areas. There is also a tendency for the thickness to increase slightly further towards the river, probably to compensate for the slope towards the water. Additional input regarding the thickness of the fill material can be found in the resistivity profiles, and thus the version of the fill layer found in model 2 and 3, i.e. FV-II, are slightly different from the FV-I (see Appendix F, **Figure 36** and Figure 38).

The characteristics of the fill material are described in the borehole logs, as being everything from silty clay, as to be consisting of sand and gravel. Broken bricks and rests of glass have also been found (Engdahl et al, 2010). The heterogeneous composition results in a great variation in the hydrogeological parameters such as hydraulic conductivity. For all simulations, what is assumed to be reasonable mean values for the observed materials are set for the entire area. The values, which are between those of sand and clay, are presented in Table 8.

Table 8. The hydraulic parameters of the fill material used in the simulations. These are horizontal hydraulic conductivity (K_H), vertical hydraulic conductivity (K_V), specific yield (S_y) and specific storage (S_s)

Geological unit	K_H (m/s)	K_v (m/s)	S_y	S_s (1/m)
Fill	$1 \cdot 10^{-5}$	$1 \cdot 10^{-6}$	0.05	0.001

4.5.2 Peat

The peat, and other organic sediment, within the updated area are interpreted as accumulated river deposits and are therefore assumed to follow the stretch of the river and the thickness is likely to decrease proportional to the distance from the river. The greatest thickness is found within the wetland where the layer of peat and mud is at least 10 meters thick according to the geological profile presented in *Engdahl et al* (2011) (see Figure 4). The borehole logs found in *Engdahl et al* (2010) gives a good idea of the extension of the peat layer. No peat has been observed in the boreholes west of the contaminated site (see Appendix F, Figure 41). No additional information regarding the thickness of the peat was derived from the resistivity profiles, hence the model of the geological layer peat (PV-I) are the same in all three geological models. As for the hydraulic parameters of the peat layer, they remain unchanged for all models (see Table 7).

The main difference between interpretation of the peat layer in the original model and the update is the thickness in the area of the wetland. In the original model, the thickness reaches a maximum of 2-3 meters whereas the thickness is much greater in the updated version (see Appendix F). However, in both versions the peat is distributed along the river but, it has been possible to, with the increased resolution and the new data create a finer description of the distribution of peat in the area.

4.5.3 Clay

In the original model, the clay layer is described as a coherent layer with an almost constant thickness of 5 meters within the area of the update. According to the boreholes logs, the thickness of the clay layer varies from 0 to 16 meters over the area, which results in an updated layer, i.e., CV-I, very unlike the original (see Appendix F, Figure 43). Based on three borehole logs with no observed clay, the updated version of the clay layer includes an area without clay to the west of the contaminated site. Another difference is the area east of the contaminated site with thicknesses up to 16 meters (see Appendix F, Figure 44).

4.5.4 Till

In the original model the till layer has a constant thickness of around 10-11 meters within the area of the update (see Appendix F, Figure 46). In general this is greater than what has been observed in most boreholes. As compared to the overlying geological layers, there is less data on the layer thickness for the update based solely on boreholes logs, since only eight out of the 21 boreholes extended to the underlying limestone. Despite of the small amount of available data about the till layer, it is reasonable to assume that the layer is more varying than the original model claims. Figure 47 illustrates the first update of the till layer, i.e., TV-I, which is based on borehole logs and the geological profile in Figure 4.

As mentioned earlier there is plenty of additional information to model when also regarding the resistivity profiles presented by *Lumetzberger* (2014). In all profiles, formations that can be interpreted as local depressions in the limestone can be seen. Looking at them in a 3D-figure, projected onto an orthophoto (see Appendix B), they may all be interpreted as a 2D representation of an extended depression, stretching north to south in the area. Many questions regarding the potential depression still remain unanswered. A suggested hypothesis put forward in this thesis is that the depression is a sub-glacial channel, formed through river erosion, and

which has been filled with till during the most recent glacial period. Another plausible explanation is that the depression is an extended sinkhole, caused by slow chemical erosion (karst processes) over a very long period of time.

The geometry of the depression is uncertain and many assumptions are made in the modelling. In this thesis the depression is modelled with a maximum depth of around 50 meters in. Furthermore, it is assumed to level out in the north and south of the updated area to match the surrounding levels of the limestone in the original model.

Another uncertainty is the hydraulic properties of the material in the depression, as there is little available data on the composition of material. It is possible that it is filled with material largely resembling the overlying till, or that it is, at some locations, far more permeable due to open structures, or cavities, formed in the erosion processes. Due to these uncertainties, two different scenarios of compositions in the depression are modelled. The two scenarios, defined in TV-II and TV-III, use two different sets of hydraulic parameters (see Table 9), whereas the geometry of the depression is the same. In TV-II, the parameters for till that are already used in the area, is also used in the depression. TV-III instead models a scenario where the depression is highly permeable, using a much higher hydraulic conductivity. This represents a worst-case scenario, with regards to contaminant transport.

Figure 49 in Appendix F illustrates the updated geometry of the layer TV-II and TV-III, where a depression may be clearly seen. The red dots in the figures represent data taken from the resistivity profiles.

Table 9. The hydraulic parameters for the material in the depression in the limestone which is introduced to geological model 2 and 3. In model 2 the same parameters as for till is choosen

Model	K_H (m/s)	K_v (m/s)	S_y	S_s (1/m)
2	$1 \cdot 10^{-6}$	$2.5 \cdot 10^{-7}$	0.05	0.001
3	$1 \cdot 10^{-3}$	$1 \cdot 10^{-3}$	0.05	0.001

4.6 Verification

The regional groundwater model was calibrated and verified when the model was first created between the years 1995 and 1998. The model was later updated with new information in the year 2004 and using a new version of the modelling software MIKE SHE. The model was also updated during 2010 as a new verification of the model was done. The verification included a simulation of a pumping test performed in central Kristianstad, where calculated pressure differences were compared to observed ones (DHI, 2011).

No new calibration or verification of the model or sub-model has been performed in this study. The verification performed during 2010 is considered to be sufficient and the small changes in the hydrogeology in the new model versions are simply viewed as improvements of the model.

5. Results

5.1 Update of geological model

Profiles with the updated geology are presented in Figure 20 - Figure 22. Note that the profiles originate from the numerical model in MIKE SHE, consequently the layers in the figures represent computational layers and not geological layers. The entire calculation layer 5, representing the crystalline bedrock, is not included in the figure. The layer has a total thickness of 100 meters and only the top 10 meters are included. The profiles stretch from west to east and the location of the contaminated site is marked in red. For a profile from the original model see Appendix C.

The figures show the geometry of the geology in the numerical models and the horizontal hydraulic conductivity in each computational layer. The hydraulic conductivity in the surface layer (computational layer 1) decreases towards the wetland in the east where the fill layer with relatively high hydraulic conductivity ends and the clay and peat layer increase in thickness. This is a consequence of the fact that the value in each grid is a weighted mean value of the conductivity in the constituent geological layers. Figure 20 shows the profile from the numerical model based on geological model 1. The sandstone aquifer (computational layer 4) has a horizontal hydraulic conductivity of $1.4 \cdot 10^{-4}$ m/s, and is thus the layer with the highest hydraulic conductivity.

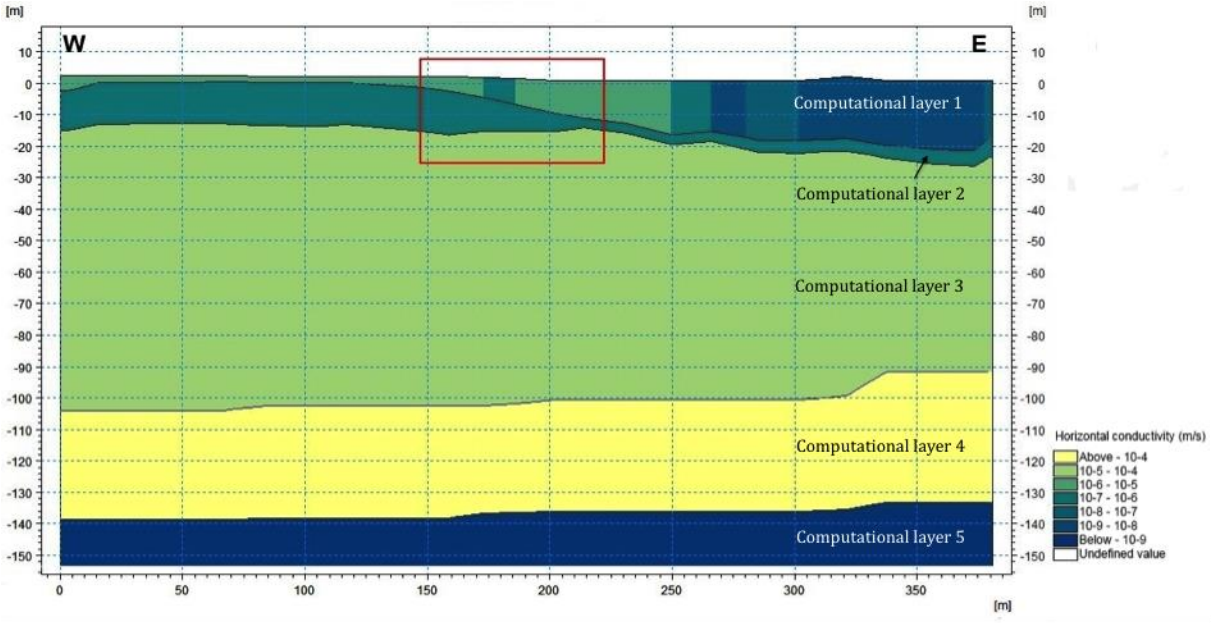

Figure 20. Profile from the numerical model generated from geological model 1. The horizontal hydraulic conductivity in each of the computational layers is also presented. The contaminated site is marked in red.

Figure 21 shows a profile from the numerical model based on geological model 2. The dominating geological feature in this model is the depression in the limestone (computational layer 3), from which a cross-section can be seen in the middle of the profile. This depression is filled with a material that has the same hydraulic properties as the overlaying till. A profile from the numerical model that is based on geological model 3 is presented in Figure 22. The geometry of the geology is the same as in the previous model. The difference may instead be found in the hydraulic conductivity of the material in the depression, which horizontally is increased from

$1 \cdot 10^{-6}$ m/s to $1 \cdot 10^{-3}$ m/s, and vertically from $2{,}5 \cdot 10^{-7}$ m/s to $1 \cdot 10^{-3}$ m/s. These parameters were chosen as to reflect a scenario where the depression has a large degree of open structures and cavities.

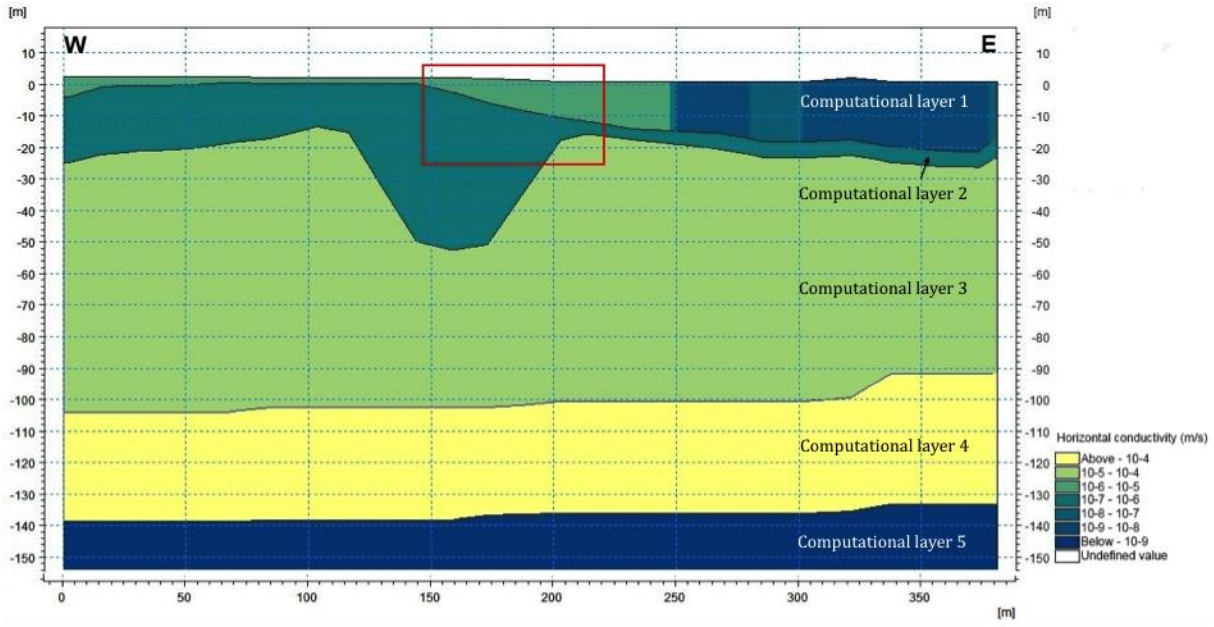

Figure 21. Profile from the numerical model generated from geological model 2. The horizontal hydraulic conductivity in each of the computational layers is also presented. The contaminated site is marked in red

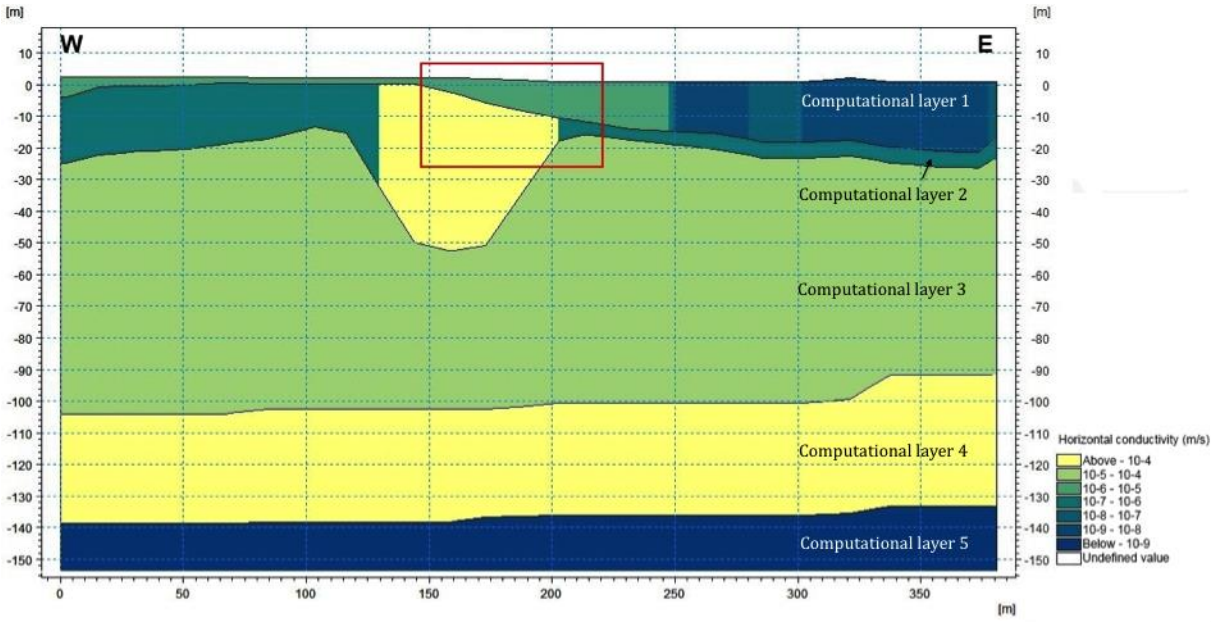

Figure 22. Profile from the numerical model generated from geological model 3. The horizontal hydraulic conductivity in each of the computational layers is also presented. The contaminated site is marked in red

5.2 Simulation results

The results from the simulation are presented so as to facilitate the analysis, which will be performed according to the flow chart in Figure 19. This means that results from the simulations of the original model and the two extraction scenarios will be presented first, followed by results from the simulations of the three updated models. The focus will be on groundwater movement within and to and from the till layer, where most of the contaminant is found, as well as on the sandstone layer, from which the great volumes of water is extracted.

5.2.1 Results from simulation 0A and 0B

Water balances for simulation 0A and 0B are shown in Figure 23 and Figure 24, respectively. They describe the accumulated flow within all processes of the model, and over the entire simulation period. The five layers in the figures do represent the five computational layers in the numerical model. The most noticeable difference between the results can be seen in the exchange flow and the boundary flow of the computational layer representing the sandstone. In the simulations with no extractions from the sedimentary bedrock (0A), the direction of the net flow between the sandstone and the limestone is directed upwards (see Figure 23), whereas with the extractions of today (0B) the net flow is almost three times bigger and directed in the opposite direction (Figure 24). The net flow into the sandstone from the sides has also increased and this with more than four times. It should also be noted that the downward flow from the layers on top of the sandstone has increased, and that the upward flow has decreased significantly with the extractions, and consequently the extractions have more or less influenced the groundwater flow in all layer within the sub-model area.

With the intention of mapping out where within the sub-model area the greatest influence of the extractions can be seen, the difference in hydraulic head (m) between the till and the sandstone is compared for the same two simulations. To begin with, the mean hydraulic head (m) over the ten years was calculated in both layers. The mean hydraulic head in the sandstone layer was then subtracted from the till layer giving the mean difference in hydraulic head between the two layers. The resulting layer shows the direction, and to some extent the relative size, of the vertical gradient. The result is presented in Figure 25 and Figure 26. Negative values, marked as red, indicate an upward gradient whereas positive values, marked as blue, indicate a downward gradient.

The only difference between the first two simulations is the added extractions in simulations 0B. By comparing the two figures it becomes clear that the groundwater extractions in central Kristianstad have had a huge impact on the direction of the groundwater flow in the surrounding area. Before the extractions from the sedimentary bedrock started, practically the whole sub-model area had an upward hydraulic gradient and was a discharge area (see Figure 25). The increased extractions have successively decreased the hydraulic potential in the sandstone to the extent that the hydraulic gradient has flipped over and large parts of the area now function as a recharge area (see Figure 26). The greatest change has occurred in the central areas of the sub-model where the extraction wells are located.

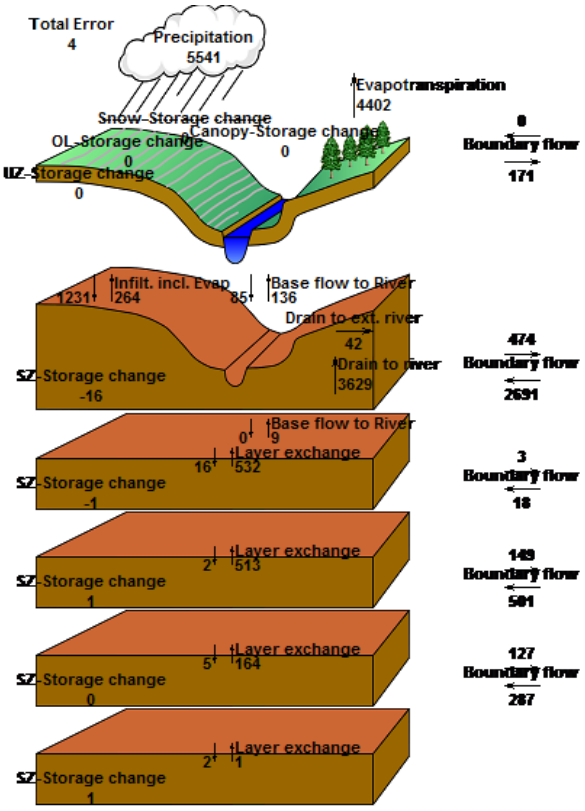

Figure 23. The water balance from the simulation with the original model and the scenario with no extractions from the sedimentary bedrock (0A). The values are expressed in mm

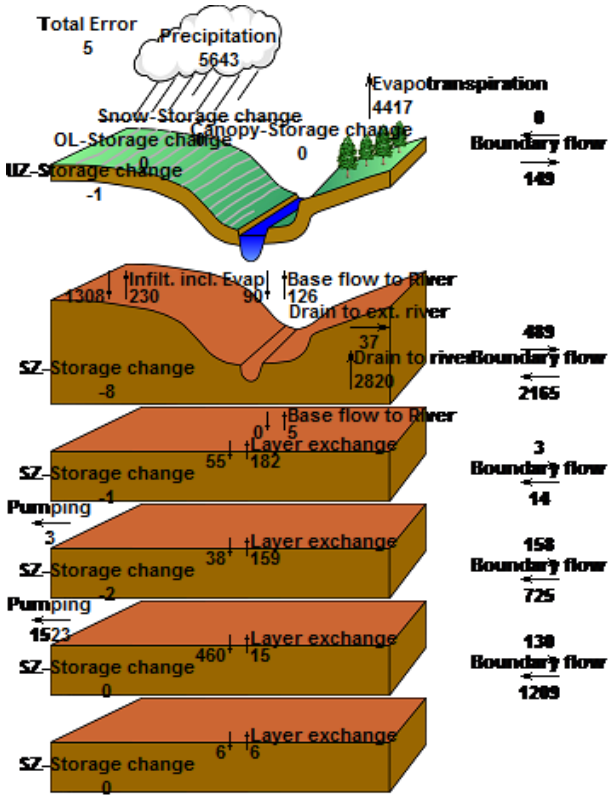

Figure 24. The water balance from the simulation with the original model and the scenario with the extractions of today (0B). The values are expressed in mm

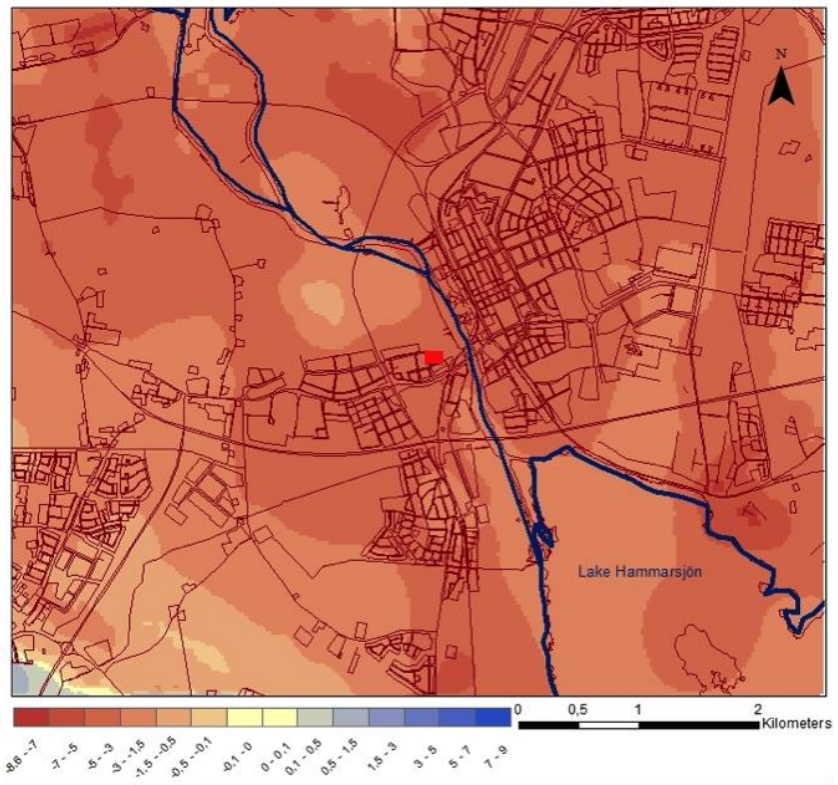

Figure 25. Difference in hydraulic head (m) between the till layer and sandstone layer. The figure shows a mean over the whole simulation period. Simulations are performed using model 0 and extractions scenario A. The location of the contaminated site is marked with a red box in the centre of the figure

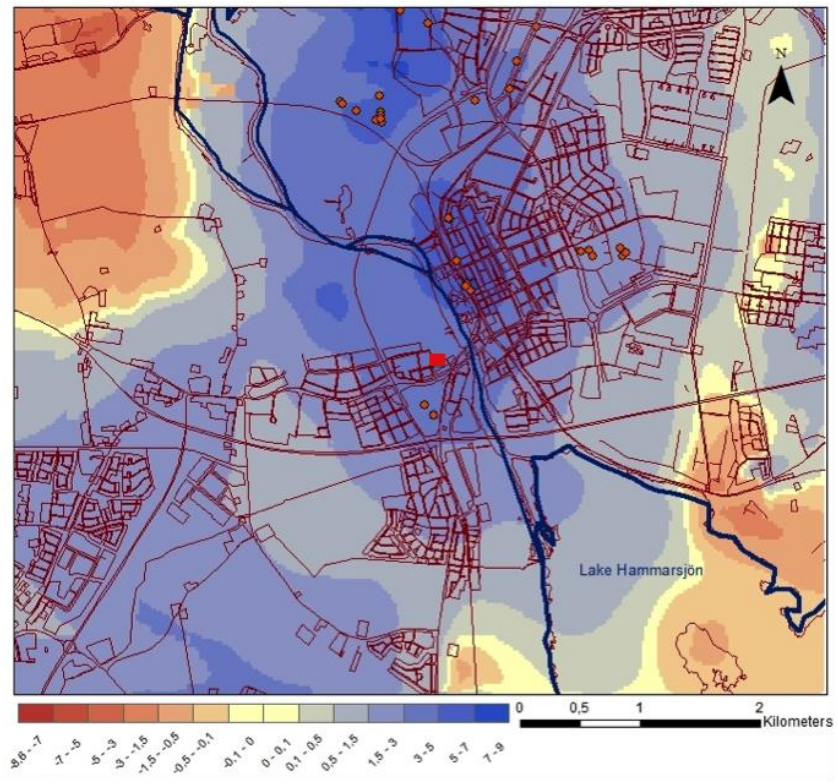

Figure 26 Difference in hydraulic head (m) between the till layer and sandstone layer. The figure shows a mean over the whole simulation period. Simulations are performed using model 0 and extractions scenario B. The pumping wells in the area are shown as orange dots and the location of the contaminated site is marked with a red box in the centre of the figure

The figures show the mean difference in hydraulic head between the two layers calculated over the entire simulation period of ten years, however the difference varies over the year. The variation can be explained by the change in season and the largest difference in hydraulic head, and thus also the largest vertical gradient, is likely to occur during the winter months. Increased infiltration, due to an increase in precipitation and a decrease in evapotranspiration, gives in an increase in groundwater potential, mainly in the upper most layers whilst the groundwater potential remains unchanged in the lower layers.

In Figure 27 to Figure 30, the mean hydraulic head in the sandstone layer and the till layer are presented. In these figures, the hydraulic head is presented using equipotential lines, where there is a difference of one meter between each line. The figures are used to predict the horizontal direction of the groundwater flow, this being perpendicular to the equipotential lines. Figure 27 shows the hydraulic head in the sandstone before the extractions from the aquifer started (simulation 0A). As may be expected, the direction of the flow is towards the Lake Hammarsjön in the southeast corner of the sub-model area, which acts as a natural discharge area, and further on, in the direction towards the sea. The effects of the extractions from the sedimentary bedrock on the hydraulic head in the sandstone can be seen Figure 28 (simulation 0B). With the extractions of today the groundwater flow is completely altered and is now directed towards the extraction wells. The denser equipotential lines indicate a steeper hydraulic gradient. Furthermore, the simulation results show that the mean hydraulic head in the area adjacent to the municipal wells in central Kristianstad is decreased with more than 13 meters.

Figure 29 and Figure 30 show the mean hydraulic head in the till layer for simulation 0A and 0B, respectively. As in previous figures, two equipotential lines denote a difference of one meter in mean hydraulic head. Comparing the two figures, it becomes clear that the extractions from the sedimentary bedrock have a substantial impact on the groundwater potential in overlying soil layers. Within the area of the extractions the mean hydraulic head has decreased with around 3 meters.

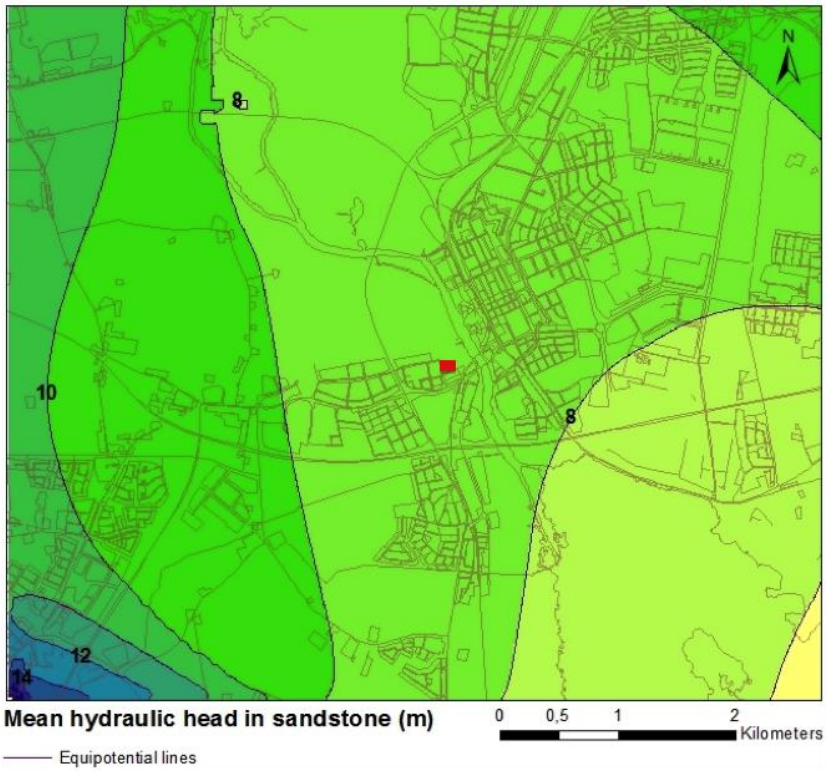

Figure 27. Mean hydraulic head (m) in the sandstone layer (referens sea level). Results from the simulation with unchanged model and the scenario with no extractions (0A). The location of the contaminated site is marked with a red box in the centre of the figure

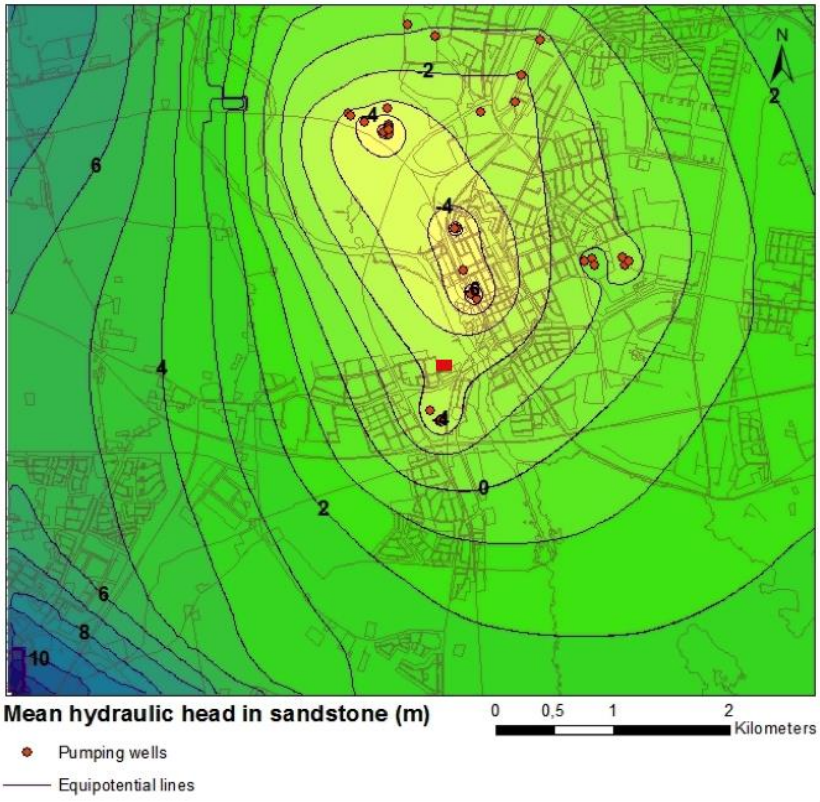

Figure 28. Mean hydraulic head (m) in the sandstone layer (referens sea level). Results from the simulation with the unchanged model and the scenario with the groundwater extractions of today (0B). The pumping wells in the area can be seen as orange dots and the location of the contaminated site is marked with a red box in the centre of the figure

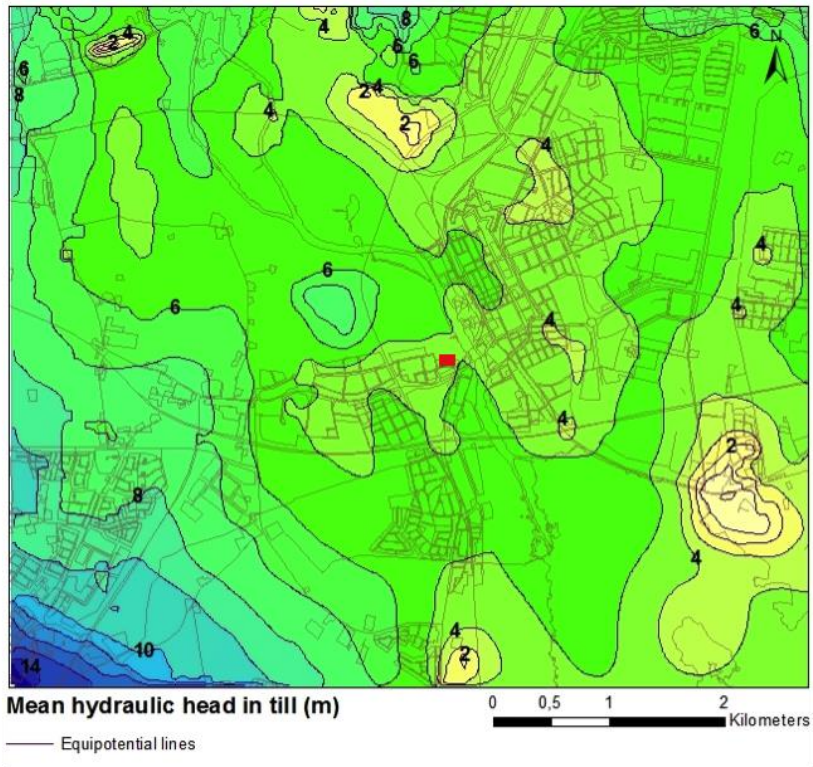

Figure 29. Mean hydraulic head (m) in the till layer (referens sea level). Result from the simulation with the unchanged model and the scenario with no extractions (0A). The location of the contaminated site is marked with a red box in the centre of the figure

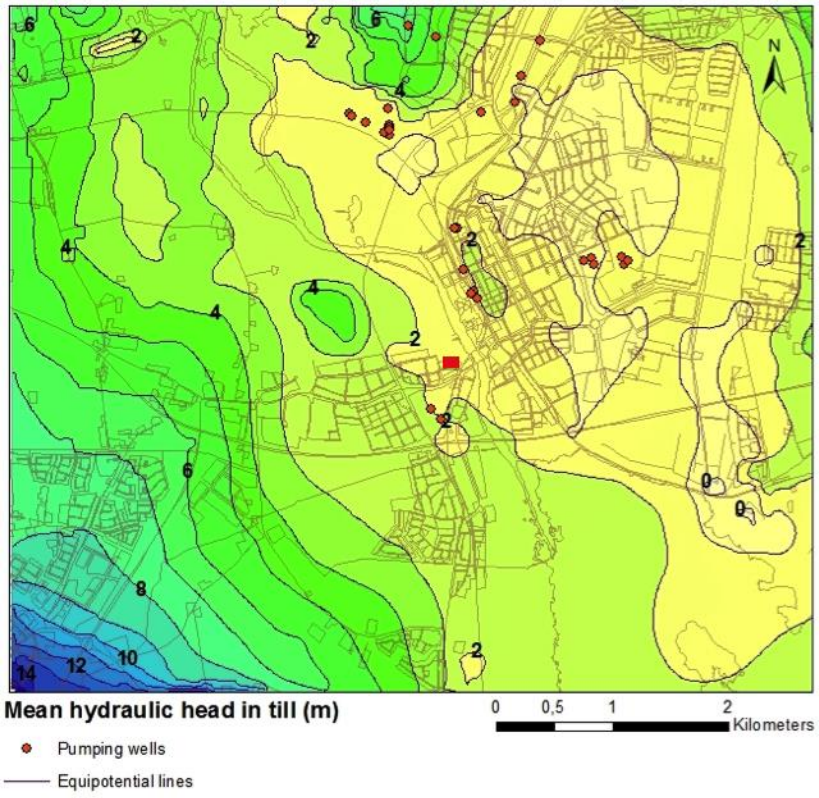

Figure 30. Mean hydraulic head (m) in the till layer (referens sea level). Result from the simulation with the unchanged model and the scenario with the groundwater extractions of today (0B). The pumping wells in the area can be seen as orange dots and the location of the contaminated site is marked with a red box in the centre of the figure

Figure 31 and Figure 32 shows the same result as in the previous two figures, but gives a close up of the area around the contaminated site, which can be seen in the centre of the figure, marked by the red polygon. The difference between the equipotential lines in these figures is decreased to 0.5 meter. Generally, it can be said that the variations in hydraulic head in the till layer follows the variations in the topography to some extent. Note, e.g., the shapes in the northwest part of the figures. This elevation in hydraulic head corresponds to an elevation in the landscape, more precisely the closed landfill site Härlövsdeponin. The same elevation can be seen in centre of Figure 29 and Figure 30. For a topographic map of the sub-model, and for the close up of the area around Färgaren, see Appendix D and Appendix E.

From the Figure 31, the general flow direction without extractions may be determined. The horizontal gradient is directed from a hydraulic head of 7.5 meters in the west towards the river, and then further on to 4.5 meters in the east of the figure. This results in a groundwater flow in the same direction, following the decrease in elevation towards the river, and then further on to the lowest point within the sub-model area, which is located in the east part of Kristianstad (see Appendix D).

In Figure 32, the change followed by the extractions of the area can be seen. As also noted earlier, the hydraulic head has decreased substantially due to the extractions from the sandstone, and in the local area around Färgaren by as much as 3 to 3.5 meters. The extractions have thus most likely increased the vertical gradient in the till. Moreover, alterations of the horizontal groundwater flow directions in the till may also be observed in the area. The main flow direction is still towards the east and the lowest point within the sub-model, although the flow in the north part if the area is directed towards the river. Seen from the site Färgaren 3, the local flow direction is towards the north-northeast. It is also of interest to note that the industrial wells south of the contaminated site seem to have little impact on the local groundwater flow directions in the till.

5.2.2 Results from simulations 1B, 2B, and 3B

The update of the area around Färgaren has shown no significant effect on the overall results of the sub-model. However, local effects on the hydraulic head may be observed. The figures in this section, Figure 33, Figure 34 and Figure 35, show the mean hydraulic head in the till layer from simulations with the three updated geological model. As within previous figures of the hydraulic head in the till layer, the influence of the topography is clearly visible. Comparing the figures to the map over the topography in the area (see Appendix E), many features that may be related to the variation in elevation can be observed. As shown within the corresponding figures from the original model, the landfill in the northwest part of the area is reflected in the variation of the hydraulic head. Other elevated areas and local depressions are also reflected. Note, e.g., the two areas having slightly higher hydraulic head in the southwest and the northeast of the figures, which corresponds to local elevations.

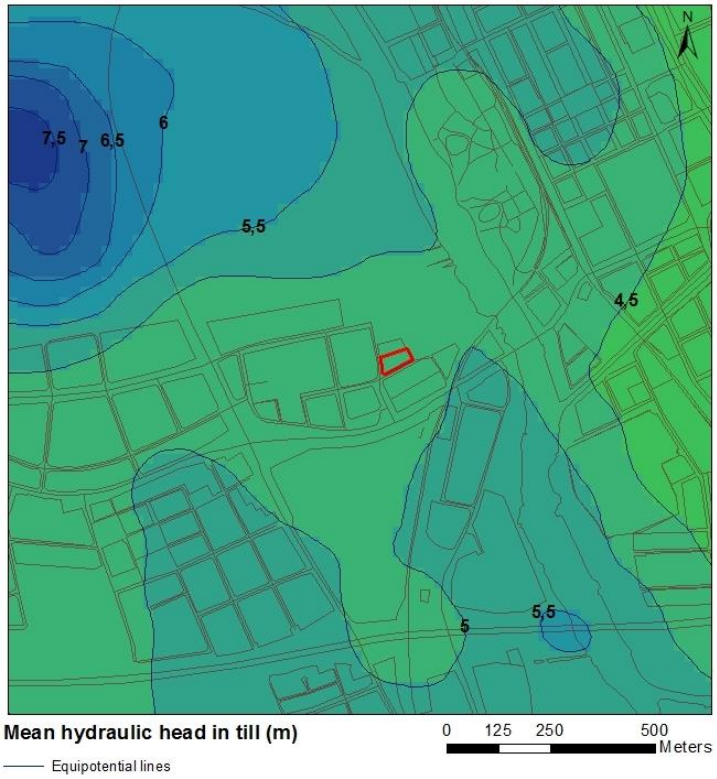

Figure 31. Mean hydraulic head (m) in the till layer (referens sea level). Close up on the area around the contaminated site, which is marked with a red polygon. Result from simulation with original model and scenario without extractions (0A)

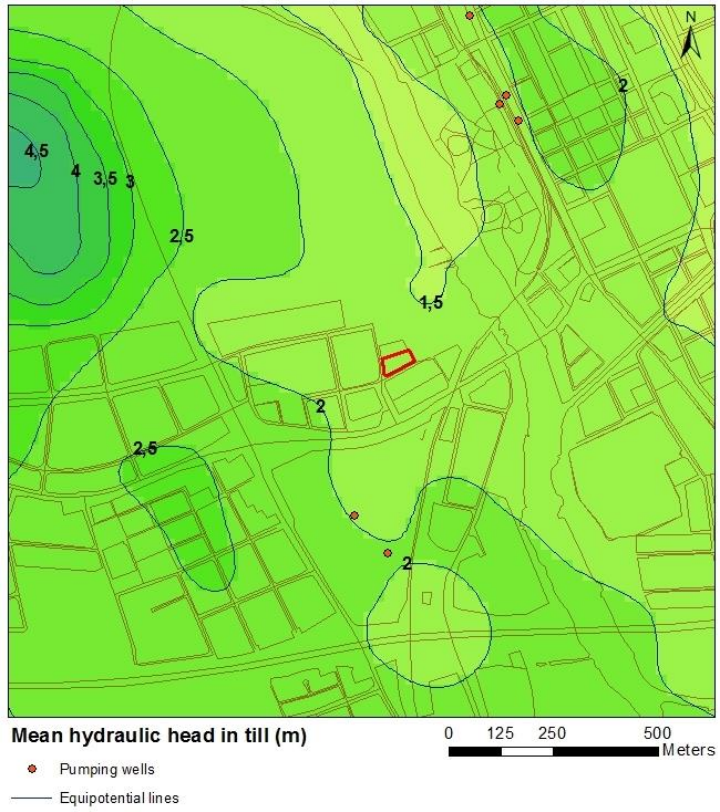

Figure 32. Mean hydraulic head (m) in the till layer (referens sea level). Close up on the area around the contaminated site, which is marked with a red polygon. Result from simulation with the original model and the scenario with groundwater extractions (0B)

When it comes to the difference the update in the geology make, the influence of the more detailed description of the clay layer seems to have been significant. The absence of clay west of the contaminated site has lowered the hydraulic head in that area substantially. Comparing the results from the original model in Figure 32, with the updated model 1 in Figure 33, the hydraulic gradient has partly changed direction, and is now also directed towards the area without clay just west of the contaminated site.

Figure 34 shows the results of simulation using the geological model 2, in which the depression has been introduced. No significant change in the groundwater flow pattern may be observed, when the results are compared to the simulation without the depression. In Figure 35 the results from geological model 3 is presented. The figure illustrates the impact of an increase in hydraulic conductivity within the depression, on the groundwater flow pattern in the till. The direction of the flow is in large part of the area directed towards the depression.

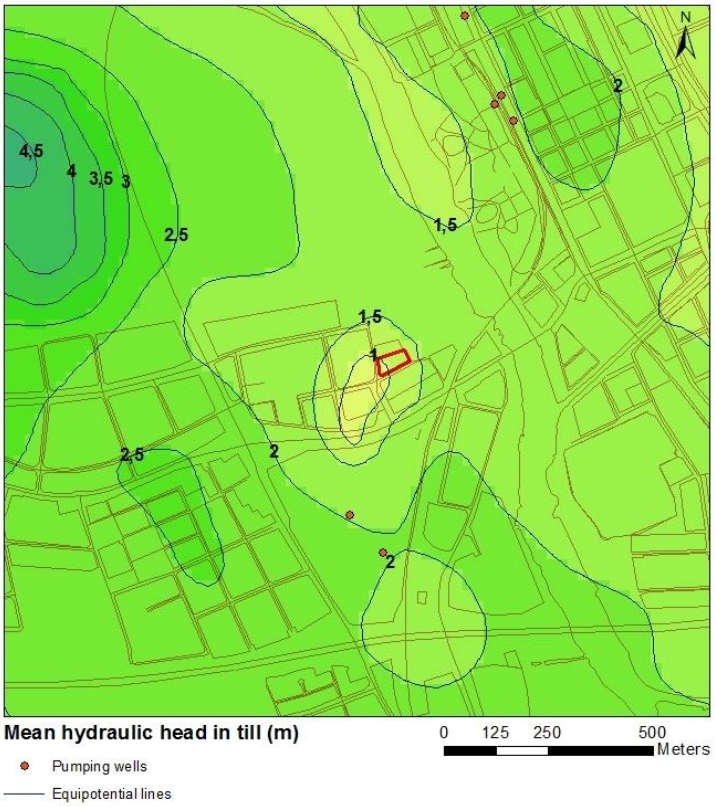

Figure 33. Mean hydraulic head (m) in the till layer (referens sea level). Close up on the area around the contaminated site, which is marked with a red polygon. Result from simulation with the updated model 1 and with extractions (1B).

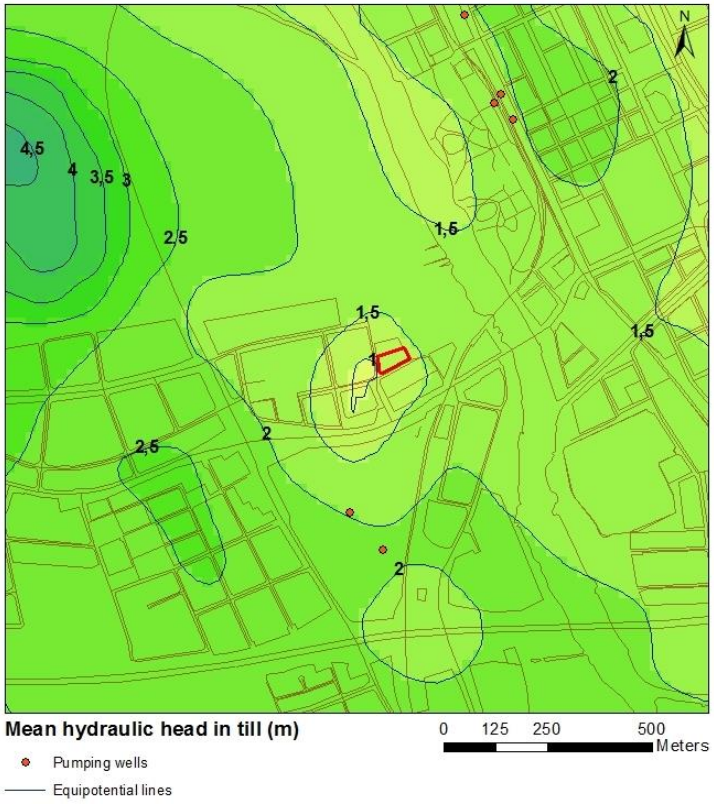

Figure 34. Mean hydraulic head (m) in the till layer (referens sea level). Close up on the area around the contaminated site, which is marked with a red polygon. Result from simulation with updated model 2 and with extractions (2B).

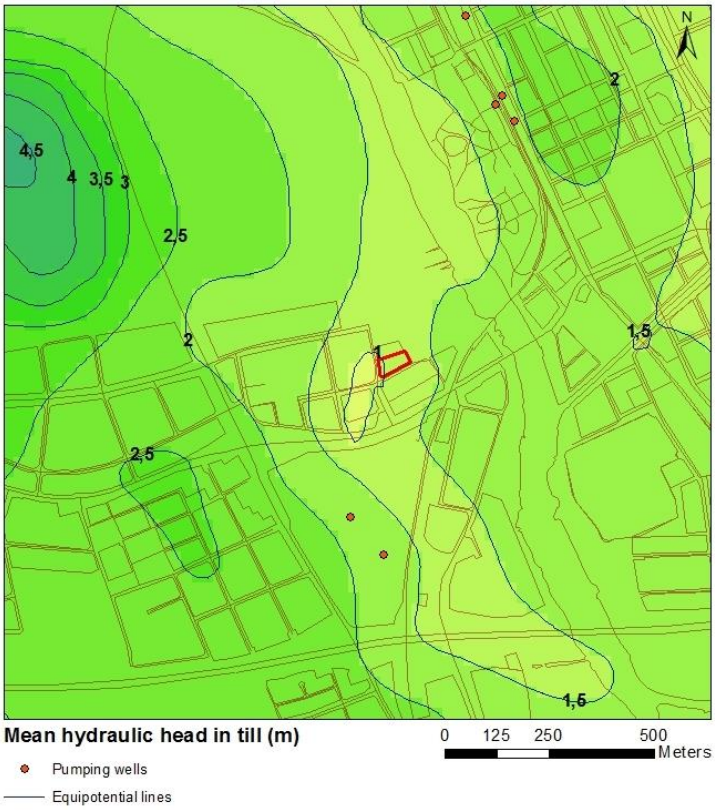

Figure 35. Mean hydraulic head (m) in the till layer. Close up on the area around the contaminated site, which is marked with a red polygon. Result from simulation with updated model 3 and with extractions (3B).

6. Discussion

6.1 Groundwater flow variations in time and space

The discussion takes its starting point in the first box in Figure 19, i.e., commences by viewing the groundwater flow variation in the sub-model area over the twentieth century. The two scenarios 0A and 0B, can be seen as two snapshots that illustrates the groundwater flow from the situation in the early twentieth century, as compared to a more present situation. What is evident from the background check is that the extraction has greatly increased over time, and therefore, examining a change over time is equivalent of examining a change by increased extraction. The increase in extraction has likely been gradual as more industries were established in the area, and as Kristianstad has become more populated. The changes in groundwater flow have therefore likely also been gradual.

The increased extraction in the area has had several effects on the hydrogeological situation, and some of them, hopefully the most important, have been accounted for in this thesis. The greatest change has happened in the sandstone layer, from where most of the water is extracted. For this layer, the vertical net flow towards the overlying limestone has changed direction, and instead of leaving the layer, the groundwater is now entering it, at a three times larger degree than before. The flow mainly originates from the limestone, but there is also an increased flow from the overlying soil layers. This indicates that the sandstone communicates with the overlying soil layers, such as the till layer. In the horizontal direction, the net flow is still directed into the sub-model area, but the volumes have drastically increased.

The vertical flow directions within the sub-model have also been studied in more detail, showing how the central parts of the sub-model has changed from being a discharge area into being a recharge area. These results coincide with the results in *Engdahl et al* (2011). Their results show that a varying, but always downward, vertical hydraulic gradient was observed between the till and the sandstone during the time of the survey. The horizontal hydraulic gradient in the sandstone is also modelled, and the results show how it has changed from being directed to the southeast, to be very clearly facing the municipal extraction wells located in central Kristianstad and at Näsby fält, north of the city. Also concluded from the results, is that the mean hydraulic head in the sandstone layer has greatly decreased in these areas as a result of the groundwater extraction. For the municipal wells in central Kristianstad, this decrease is up to 13-15 meters in the simulations.

In the soil layers, the increased extractions show some similar effects as for the lower sedimentary bedrock. As in the sandstone, the mean hydraulic head in the till layer has also decreased in the area of the extractions. However, the general flow direction in the till layer remains practically unchanged, and is directed towards the east, to the lowest topographic point in the sub-model. Local changes may though be noted. Further examining the immediate environment around Färgaren 3, the local flow direction changes from east to the north-northeast. This change may be the result of extractions in the nearby municipal wells, located northeast of the river Helge, in central Kristianstad. Due to the topography, the flow is naturally directed towards the river, and this appears to be locally enhanced further by the extractions. Moreover, no significant impact from the two industrial wells south of the site is seen. These results differs somewhat from the results shown in *Engdahl et al* (2011), who concluded the main flow directions to be towards the east, and the southeast.

6.2 The importance of detailed hydrogeology

The discussion now moves onto the second box of Figure 19, performing a sensitivity analysis of the MIKE SHE groundwater model, to illustrate the influence of detailed hydrogeological characterization on the model results. The initial model is regional and comprehends the entire Kristianstad basin and thus, very different in scale. When modelling such a large area, many simplifications were done, and they may be problematic as regards some aspects in this thesis. When attempting to model local variations in the groundwater flow, the initial model may not be satisfactory, being too general. The implications of this are visualised in the sensitivity analysis, by comparing results from the original sub-model with results where recent studies of local geology have been incorporated. Three updated models have been compared to the original one, all applied to extraction scenario B. These are based on two types of measured data, acquired from boreholes and resistivity measurements, respectively.

In general, the results from the updated models locally show a significant difference from the original model, around the contaminated site. Some updated layers seem to have larger impact than others, and they will be the main focus of the further discussion. One such layer is the clay layer, which in the original sub-model around Färgaren is simplified and evenly distributed with a thickness of around 5 meters. Detailed information from borehole logs show a much more varying thickness, which incorporated into the updated models has a significant effect on the groundwater flow directions in the till layer. The effect is largely due to the very low permeability of the clay. This means that when the large extractions created a strong downward vertical gradient, this also gave a horizontal hydraulic gradient towards areas of greater permeability, i.e., where the clay layer is thin. Therefore, having a detailed model of the clay is important, as it affects groundwater movements both vertically and horizontally. The update is locally limited to the zone around the contaminated site, but an extended update would likely have a large impact on the entire sub-model. This could potentially also improve the results, and thus the understanding of contaminant transport.

In the limestone layer, a potential north-south aligned depression has been indicated in recent resistivity measurements. It is supposed that the depression likely consists of till, being the layer overlying the limestone, but may also have other features affecting the hydrogeology. This spatial heterogeneity could be open structures or cavities, which would result in an increased hydraulic conductivity in limited parts of the depression, so called preferential flow paths. The two versions of the depression being incorporated into the model show quite different results, and further studies should be undertaken in order to understand the existence and composition of the depressions better. In the version, where it is assumed to be composed of homogeneous till, it does not affect groundwater flow significantly, but may still affect the spreading of the contaminant. The version with high degree of open structures, represented by high hydraulic conductivity in the material of the depression, seems unrealistic as the result shows huge effects on the groundwater flow patterns. Such changes would probably have been observed in other studies. A more realistic alternative is that composition is likely to vary along the depression.

6.3 Contaminant transport in the area

The concluding discussion, will in accordance with Figure 19, treat contaminant transport in the area around Färgaren 3. The spreading of a contaminant in nature is governed by many different factors. Some are connected to the chemical and physical properties of the contaminant itself, such as density, solubility, degradability and the tendency to sorb to soil. Others are connected to the groundwater and the groundwater flow directions. These are in turn indirectly governed by, e.g., extraction levels and geological features in the area. Another aspect is the toxicity of the contaminant, which determines the extent of the negative effect of the spreading.

PCE is a chemical that has higher density than water, i.e., it tends to sink vertically until it reaches a layer of sufficiently low permeability, where it either stays or is further transported horizontally. More specifically for Färgaren 3, where a depression may be seen in the underlying sedimentary bedrock, this means that the contaminant may potentially travel to great depths. Moreover, the clay layer thins out and disappears completely in the west part of the contaminated site, which corresponds to the most highly contaminated area. Thus, a layer that would typically reduce the transport of PCE is missing, and therefore the risk of vertical transport is increased. Furthermore, PCE has quite low solubility in water, just as other chlorinated solvents. The effects of this are both positive and negative from a contamination perspective. PCE dissolves slowly and is thus released into the groundwater at low levels, while the contamination will persist during a long time. Even if the dry cleaner has not been in operation since 1988, high concentrations of PCE could still remain unsolved in the soil at the site. It will thus operate as a secondary source, which will continue to pollute the groundwater if not removed.

To motivate the importance of mapping how the dissolved contaminant spreads, one may consider the degradation process of PCE. It is naturally degraded through reductive dechlorination at anaerobic conditions, which are common in sub-surface environment without contact to the atmosphere. In each degradation step the density decreases, the solubility increases, the tendency for sorption to the soil becomes smaller, and the degradation becomes slower. Thus, the degradation products are more inclined to be transported with the groundwater than PCE. The last chlorinated hydrocarbon in the degradation process, i.e. VC, is hence the most soluble, and least degradable degradation product. This places most likely VC in the fronts of the contaminant plumes. VC is also the degradation product that is considered the most carcinogenic and has the lowest limit values for drinking water. Evaluating the extension of the contaminant plumes carefully is therefore important.

There is a clear downward vertical hydraulic gradient between the till layer and the sandstone within the area, which is verified both by earlier observations and by the results in this study. Before, when there was less extraction of groundwater, the aquifer was to some extent protected by an upward gradient according to the results. This is not the case any longer, and the aquifer is now therefore more sensitive to human activities at the surface. There is a considerable communication between the sandstone aquifer and the overlying layers, which is also verified by earlier observations, and by the results of this study. The combination of a downward facing gradient and a communication between the layers has increased the risk of the contaminant spreading to the sandstone aquifer from the contaminated soil layers.

The interpreted plumes from groundwater sample shows spreading in the till, to the south, southeast and northwest. However, there is no data that defines the extension of the contaminant plume in the east-northeast, since no groundwater samples have been taken in that direction, i.e., in the wetland. The interpretations correspond to observed flow direction to the south and southeast. From this, concerns were raised regarding potential spreading to the industrial wells south of the site. The result from this study does instead suggest that the municipal wells in the centre of Kristianstad are at greater risk. This is because the main flow direction in the sandstone, and partly in the till, is shown to be directed towards the northeast, where the municipal wells are located.

7. Conclusion and recommendations

The simulations in MIKE SHE show that the increase of extractions from the sandstone aquifer during the twentieth century has had a major effect on the groundwater in the sub-model area. From being a discharge area, a large part of the area is now a recharge area, which increases the risk of vertical spreading of PCE. Within the sandstone, the flow direction is completely altered. The gradient has gone from being directed to the southeast, to be facing the municipal extraction wells in central Kristianstad and at Näsby fält, north of the city. The influence of the extractions is noticeable in the overlying geological layers as well. Whereas the general horizontal flow direction remains unchanged, mainly dominated by the topography and the surface water, the mean hydraulic head has decreased significantly.

Locally at Färgaren 3, the horizontal spreading direction of the dissolved contaminants in the till layer is determined to be to the east, at the time before the extensive extractions started. With today's extractions, a north-eastward directionality is also found in the results, most likely caused by the municipal wells in this direction. As no groundwater samples have been taken in the area between the contaminated site and the municipal wells, new samplings would be highly recommended to evaluate the contaminant plume. It is pointed out that these samples would only show a snapshot, and no conclusions could therefore be drawn about whether the contaminant plume is stable, growing or declining. A good idea would hence be to perform a simulation of contaminant transport in the area, to complement these results. Such simulation could indicate answer to the question of whether the contaminants will reach the nearby wells, and when.

The presence of a depression in the limestone at the contaminated site would most likely increase the vertical spreading of the PCE, both solved and unsolved. The simulations show that the influence of a possible depression on the groundwater flow in the area varies significantly with the properties of the depression. Sections with high hydraulic conductivity would significantly increase the groundwater flow, and may thus increase the extension of the contaminant plume. The potential significance of the possible depression and the many unanswered question regarding its properties is a cause for undertaking further studies.

The results of the sensitivity analysis show that detailed knowledge of the hydrogeology is of importance when it comes to modelling the groundwater flow in the area around the contaminated site. The more detailed description of the clay in the area had a significant effect on the results of the local groundwater flow directions in the upper geological layers. Updating the entire sub-model area is therefore recommended, since this could improve the possibility to correctly simulate the local groundwater situation around Färgaren 3.

References

Bank, A. 2014. *Efterbehandling av Färgaren 3, Kristianstad kommun – Underlag för bedömning av prövningsnivå.* Göteborg: Structor Miljö Göteborg AB.

Bear, J., Verruijt, A. 1987. *Modeling Groundwater Flow and Pollution.* Dordrecht, Holland: D. Reidel Company.

C4 Teknik. 2000. *Kristianstads vattenförsörjning – Förutsättningar, möjligheter och konsekvenser.*

DHI. 2005. *Dokumentation av uppdateringar av MIKE SHE-modellen för Kristianstadsslätten.*

DHI. 2011. *MIKE SHE för Kristianstadslätten – Dokumentation av modeluppdateringar.* Report number: 12801489.

DHI. 2014. *Software for water environments.* Software catalogue 2014. Hørsholm, Denmark: DHI.

DHI Software 2014. *MIKE SHE –User Manual*. Hørsholm, Denmark: DHI.

DHI Sverige and VBB VIAK. 1998. *Dokumentation av MIKE SHE-modellen för Kristianstadsslätten.*

Engdahl, D., Larsson,N., Follin, S., Wrene, R., Bank, A. 2010. *Resultatrapport, fd kemtvätt Färgaren 3*. *Report number: 314881.* Stockholm: Hifab AB.

Engdahl, D., Larsson,N., Follin, S., Wrene, R., Bank, A. 2011. *Fördjupad riskbedömning och åtgärdsutredning, fd kemtvätt Färgaren 3. Report number: 314881.* Stockholm: Hifab AB.

Englöv, P., Cox, E.E., Durant, N.D., Dall-Jepsen, J., Jørgensen, T.H., Nilsen, J., Törneman, N. 2007. *Klorerade lösningsmedel – Identifiering och val av efterbehandlingsmetod.* Report number: 5663. Stockholm: Naturvårdsverket.

Fetter, C. W. 2014. *Applied Hydrogeology.* Fourth Edition. Harlow, England: Pearson.

Gustafsson, O., Andersson, J., De Geer, J. 1979. *Sammanställning av hydrogeologiska data från Kristianstadsslätten.* Report: 12. Uppsala: Sveriges Geologiska Undersökning.

Gustafsson, A. M., Gustafsson, L. G., Winberg, S., Refsgaard, A., 1997. *Safeguarding the Kristianstad Plain groundwater resource by using the MIKE SHE model.* European Water Resources Association Conference. 1997. Copenhagen. 357-363.

Guyton, K. Z., Hogan, K. A., Scott C. S., Cooper, G. S., Bale, A. S., Kopylev, L., Barone Jr, S., Makris, S. L., Glenn, B., Subramniam, R. P., Gwinn, M. R., Dzubow, R. C., Chiu, W. A. 2014. *Human Health Effects of Tetrachloroethylene: Key Findings and Scientific Issus.* Environmental Health Perspectives. 122 (4): 325-334.

IARC (International Agency for Research on Cancer). 2015. *List of classifications in alphabetical order.* http://monographs.iarc.fr/ENG/Classification/ClassificationsAlphaOrder.pdf [2015-02-22].

Igboakwe, M. U., Achi N. J. 2011. *Finite difference Method of Modelling groundwater flow.* Journal of Water Resources and Protection. 3:192-198.

Kemikalieinspektionen. 2015. *Teknisk beskrivning av ämnet Tetrakloreten.* http://apps.kemi.se/flodessok/floden/kemamne/tetrakloreten.htm. [2015-02-07].

Kristianstad kommun. 2015. *Sanering av kemtvätten på Långebro, Färgaren 3.* http://www.kristianstad.se/sv/Kristianstads-kommun/Miljo-klimat/Avfall--atervinning/Fororenad-mark/Sanering-av-kemtvatt-pa-Langebro/ [2015-02-06].

Kueper, B.H., Wealthall, G.P., Smith, J.W.N, Leharne, S.A., Lerner, D.N. 2003. *An illustrated handbook of DNAPL transport and fate in the subsurface.* Environment Agency R&D Publication 133. Bristol: Environment Agency.

Lindgren, J., Siverson. M., 2002. *Tylosaurus ivoensis: A giant mosasaur from the Early Campanian of Sweden.* Transactions of the Royal Society of Edinburgh: Earth Sciences, 93:73–93.

Lumetzberger, M. 2014. *3-D and 2-D resistivity and IP mapping of geology and chlorinated aliphatics at Färgaren 3, Kristianstad.* Master thesis, University of Copenhagen.

Länstyrelsen Skåne. 2013. *Regionalt program för arbetet med förorenade områden 2013-2015.* Diary number: 577-22294-2013.

Nordin, A. 2014. *Lägesbeskrivning av arbetet med efterbehandling av förorenade områden.* Case number: NV-06370-13. Stockholm: Naturvårdsverket.

RAIS (Risk Assessment Information System). 2015. *Chemical profile tool. http://rais.ornl.gov/tools/profile.php* [2015-02-21].

TRUST (TRansparent Underground STructure). 2015a. *Delprojekt 2.1*. http://trust-geoinfra.se/delprojekt/2-1.html [2015-01-27].

TRUST (TRansparent Underground STructure). 2015b. *Om TRUST*. http://trust-geoinfra.se/fyra-teman.html [2015-01-27].

Vogel, T. M., Criddle, C. S., McCarty, P. L. 1987. *Transformation of halogenated aliphatic compounds*. Enviromental Science and Technology. 21:722–736.

WHO (World Health Organisation). 2011. *Guidelines for drinking water quality.* Fourth Edition. WHO.

Wiegert, C. 2013. *Application of two dimensional compound specific carbon-chlorine isotope analyses for degradation monitoring and assessment of organic pollutants in contaminated soil and groundwater.* Diss., Stockholm University

Appendices

Appendix A: Unmodified figures

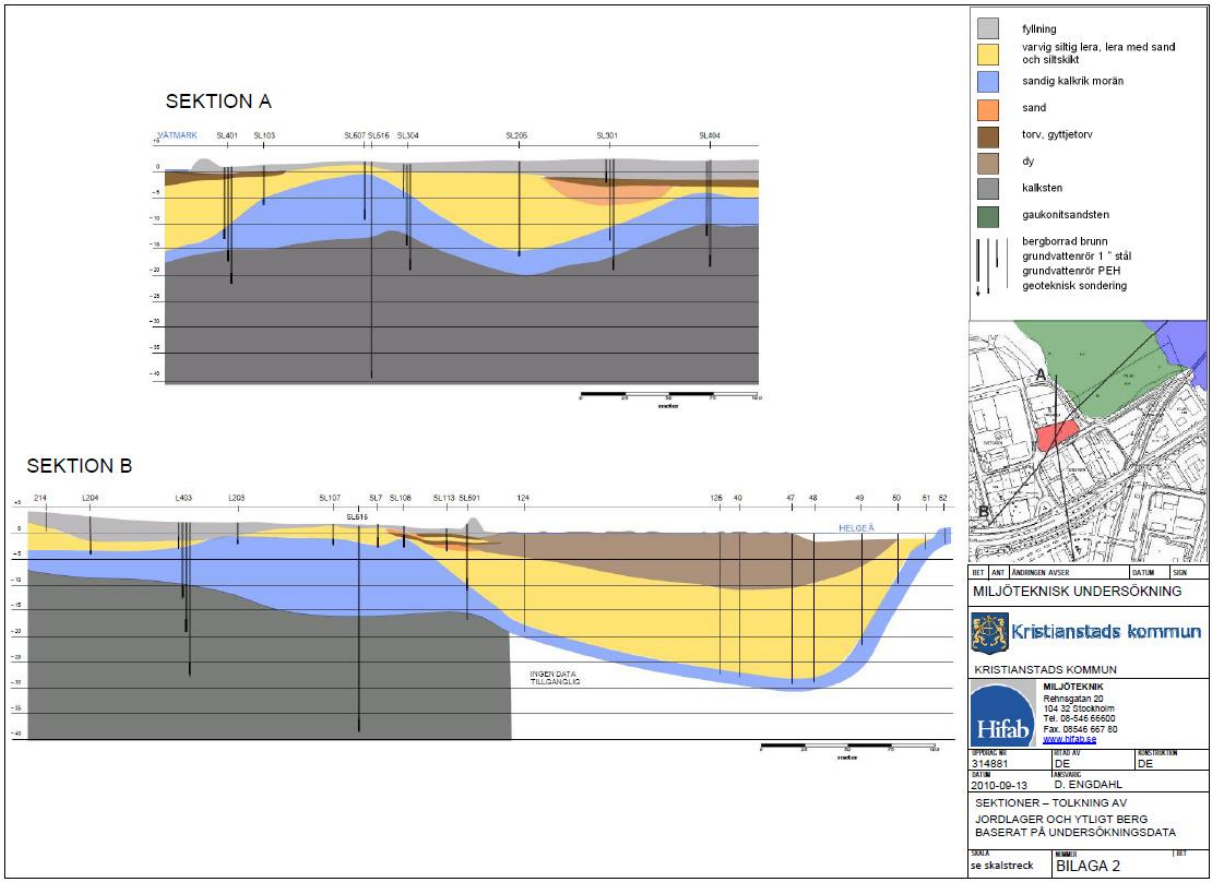

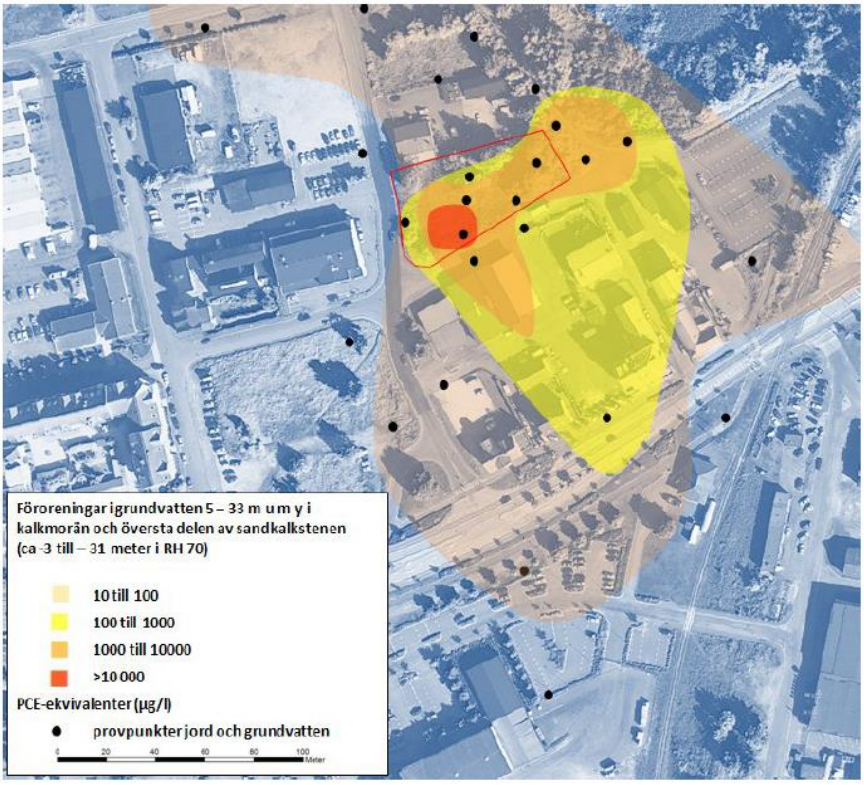

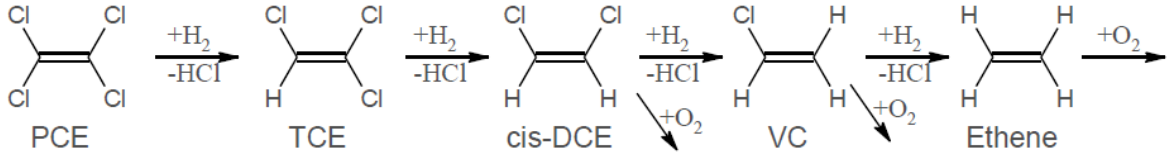
Cl
Cl
Cl
Cl
PCE
+H2
-HCl
Cl
Cl
H
Cl
TCE
+H2
-HCl
Cl
Cl
H
H
cis-DCE
+H2
-HCl
+O2
Cl
H
H
H
VC
+H2
-HCl
+O2
H
H
H
H
Ethene
+O2

Appendix B: Resistivity profiles projected onto an orthophoto

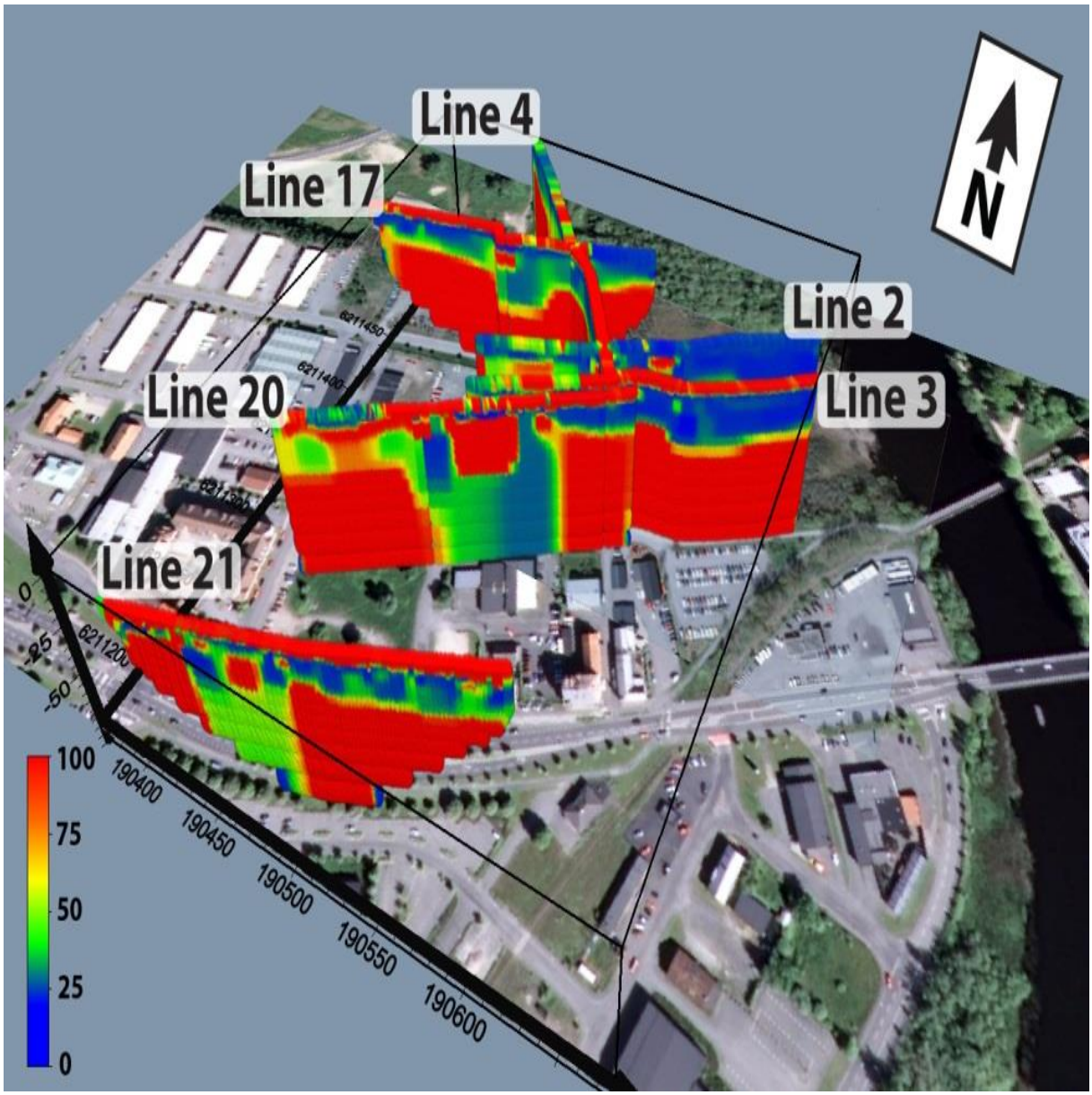

Appendix C: Geological profile from the unchanged model

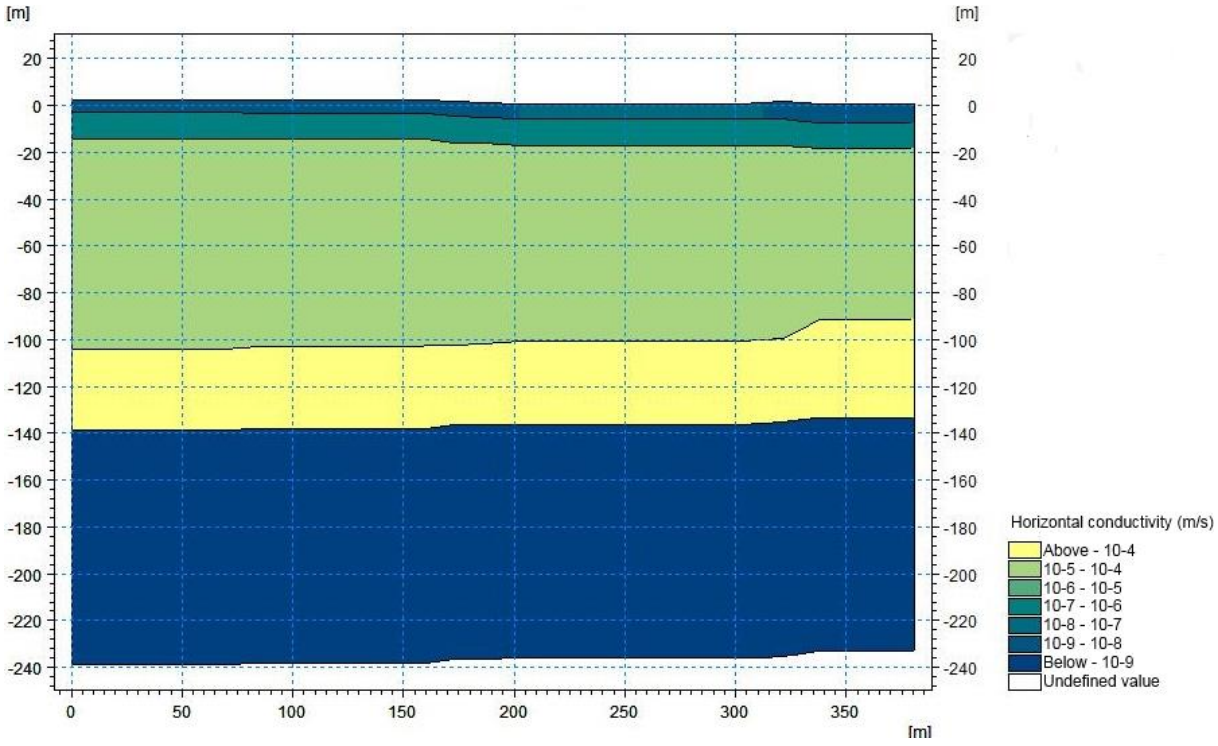

Appendix D: Topography map of the sub-model

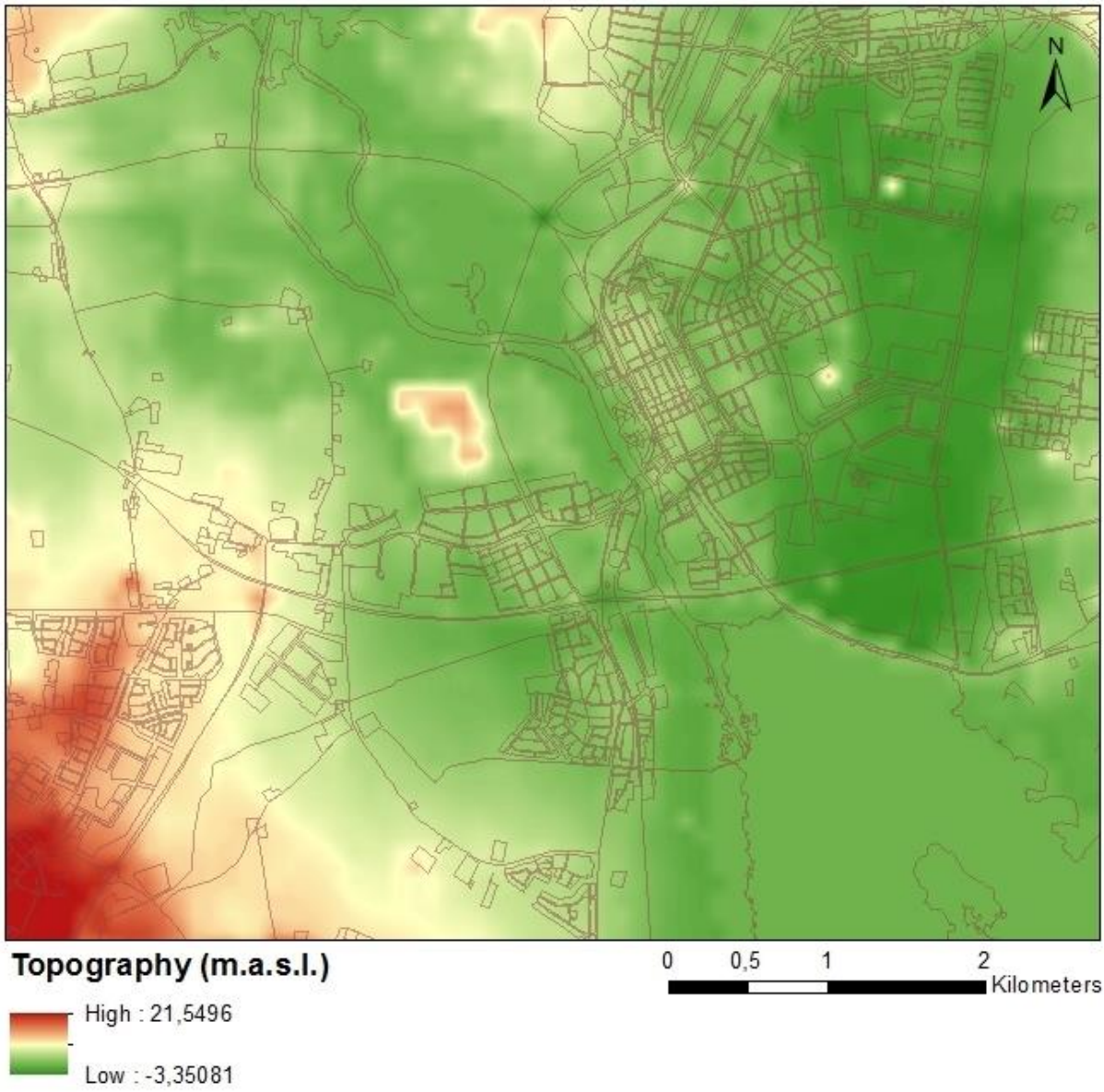

Appendix E: Topography map of the local area around Färgaren

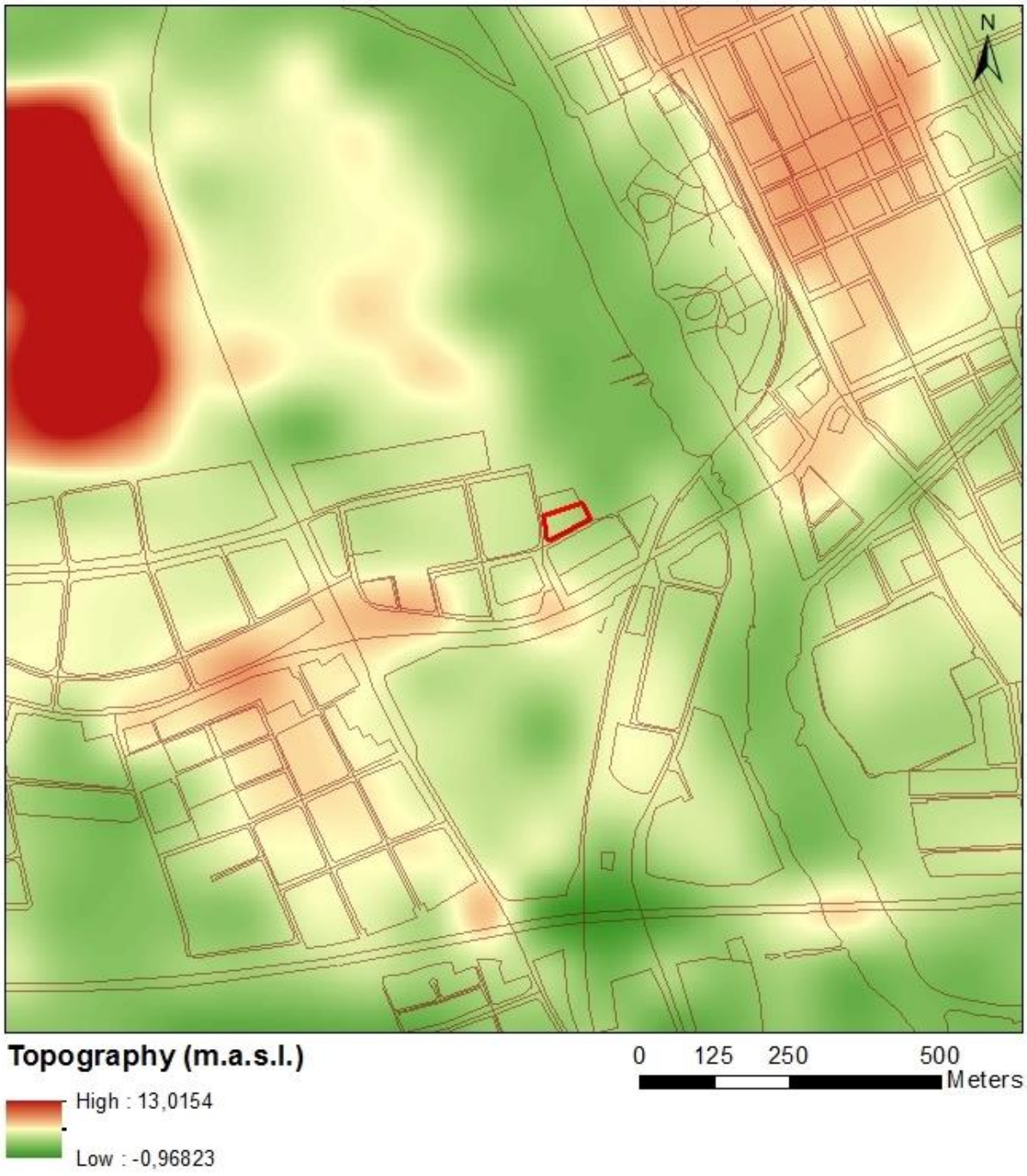

Fill version 1

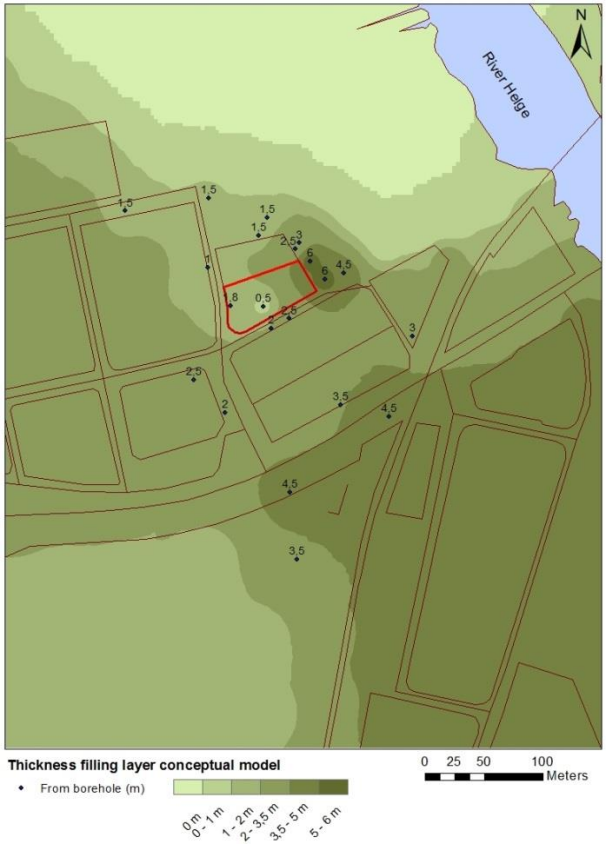

Figure 36. Horizontal overview of the thickness of the fill layer in geological model 1. The dark blue points show the location of the boreholes and attached number the observed thickness. The red polygon shows the location of Färgaren 3

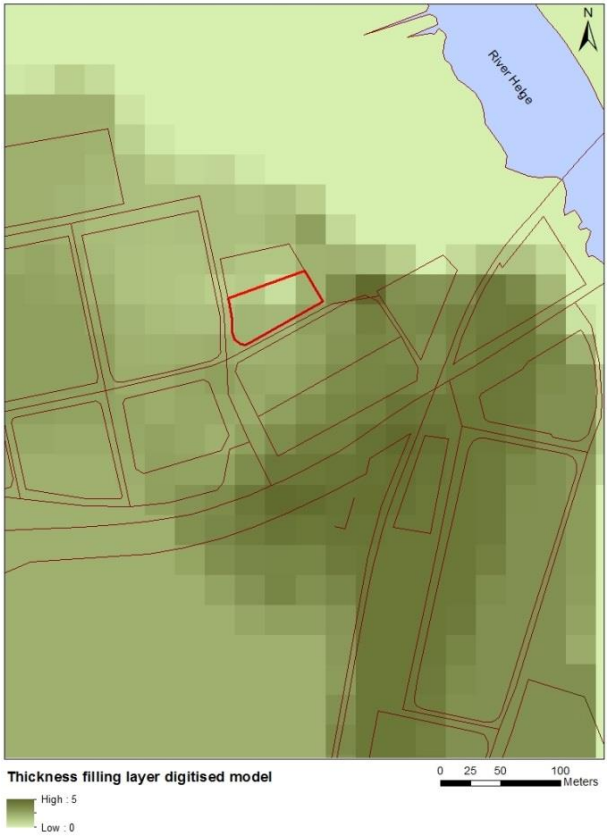

Figure 37. The digitised version of the fill layer, version 1

Fill version 2

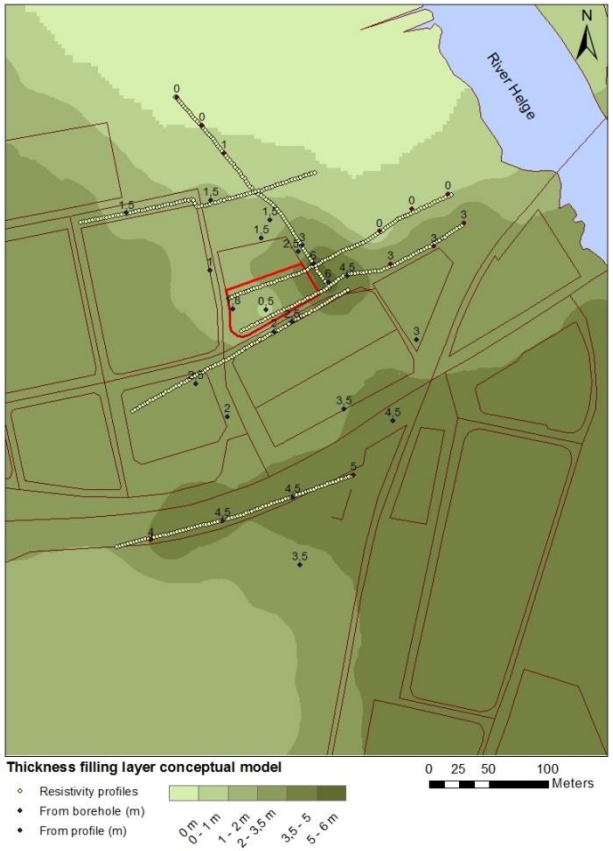

Figure 38. Horizontal overview of the thickness of the fill layer in geological model 2 and 3. The dark blue points show the location of the boreholes and attached number the observed thickness. The red points mark additional information regarding the layer thickness retrieved from the resistivity profiles. The red polygon shows the location of Färgaren 3

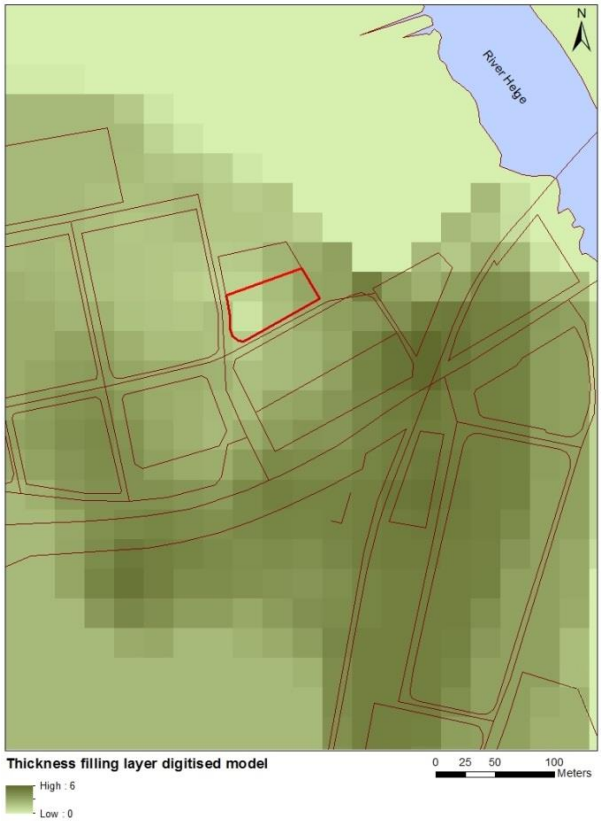

Figure 39. The digitised version of the fill layer, version 2

Peat version 1

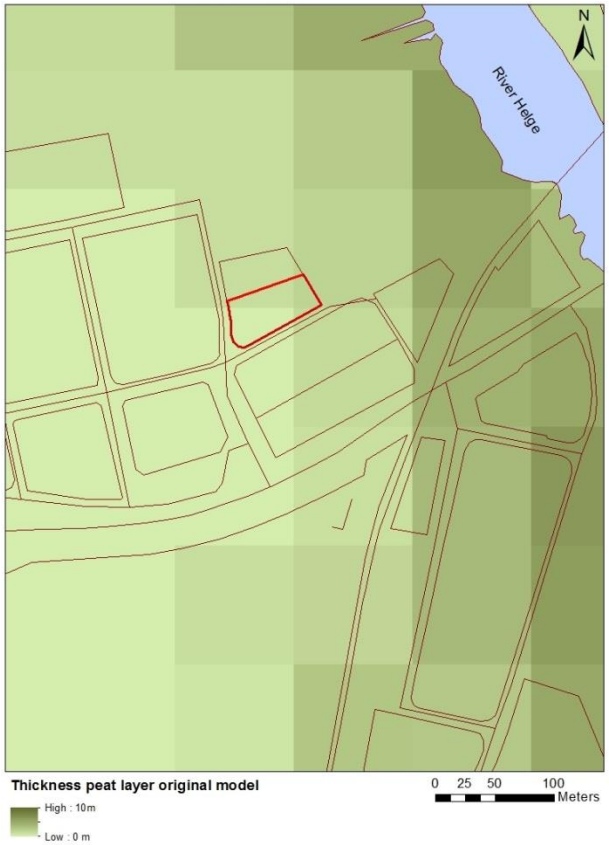

Figure 40. The thickness of the peat layer from the unchanged geological model

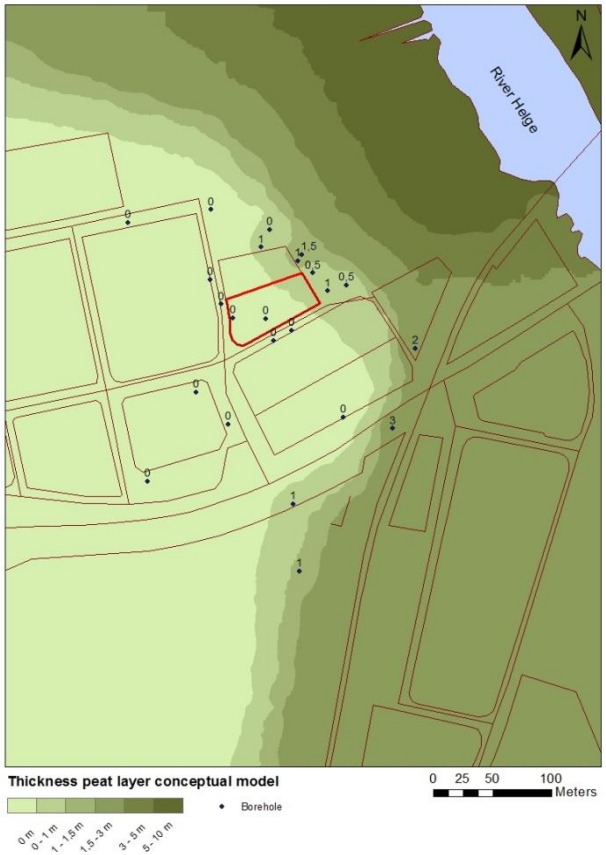

Figure 41. Horizontal overview of the thickness of the peat layer for all three models. The dark blue points show the location of the boreholes and attached number the observed thickness. The red polygon shows the location of Färgaren 3

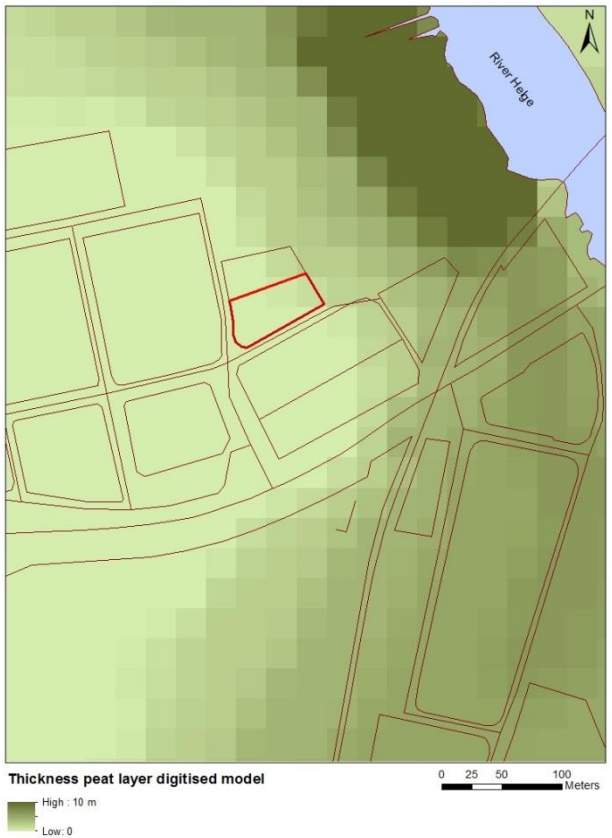

Figure 42. The digitised version of the peat layer, version 1

Clay version 1

Figure 43. The thickness of the clay layer from the unchanged geological model

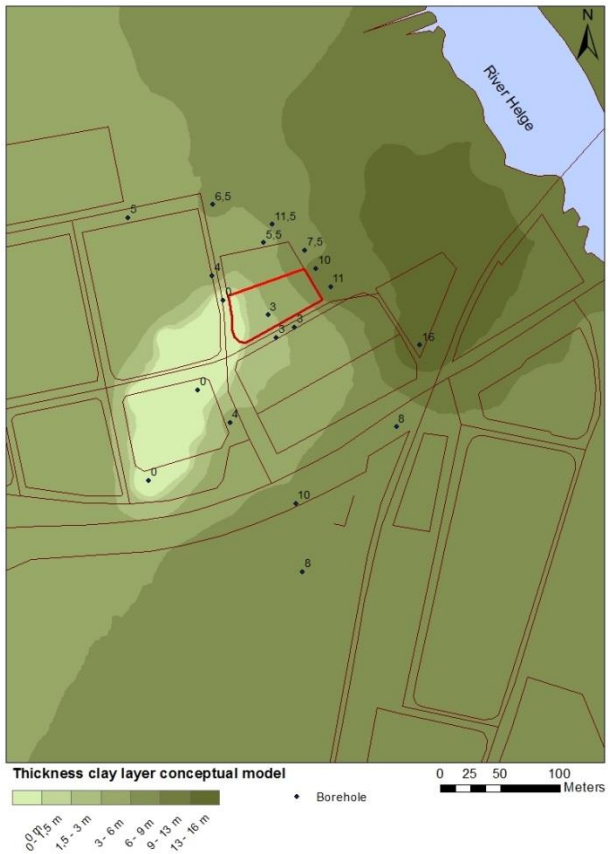

Figure 44. Horizontal overview of the thickness of the clay layer in all three models. The dark blue points show the location of the boreholes and attached number the observed thickness. The red polygon shows the location of Färgaren 3

Figure 45. The digitised version of the clay layer, version 1

Till version 1

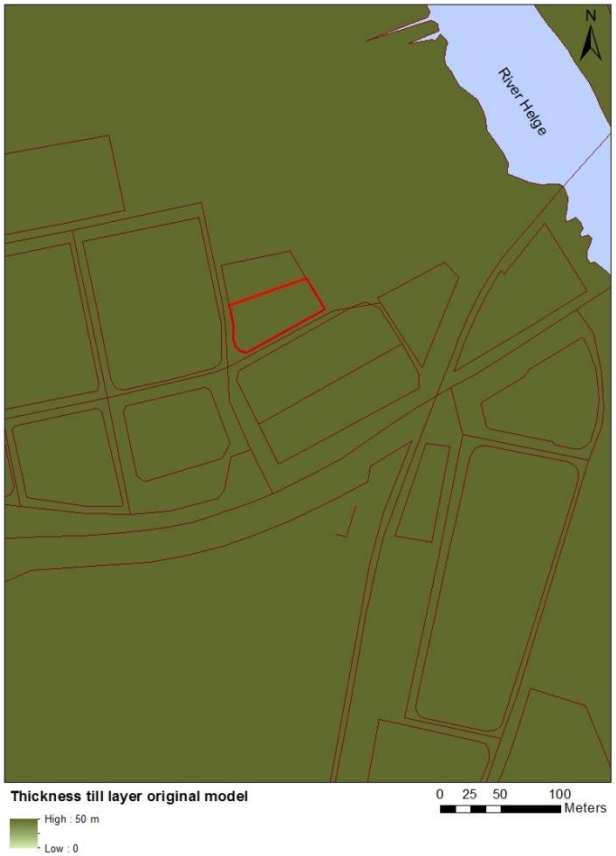

Figure 46. The thickness of the till layer from the unchanged geological model

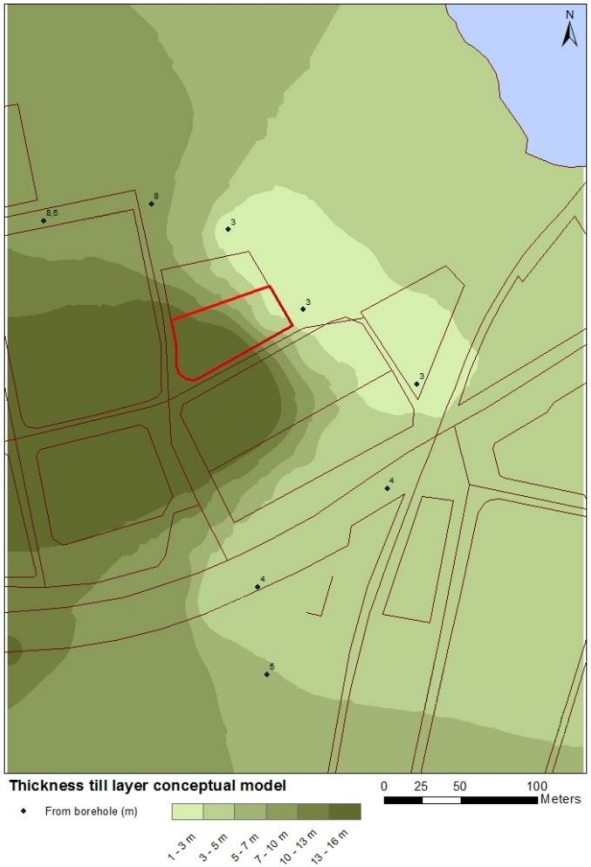

Figure 47. Horizontal overview of the thickness of the till layer in model 1. The dark blue points show the location of the boreholes and attached number the observed thickness. The red polygon shows the location of Färgaren 3

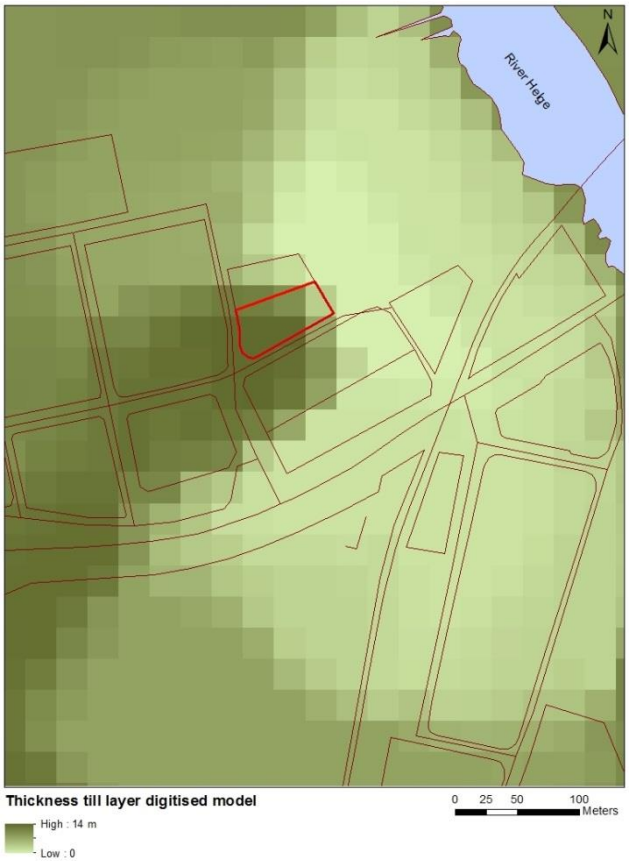

Figure 48. The digitised version of the till layer, version 1

Till version 2 and 3

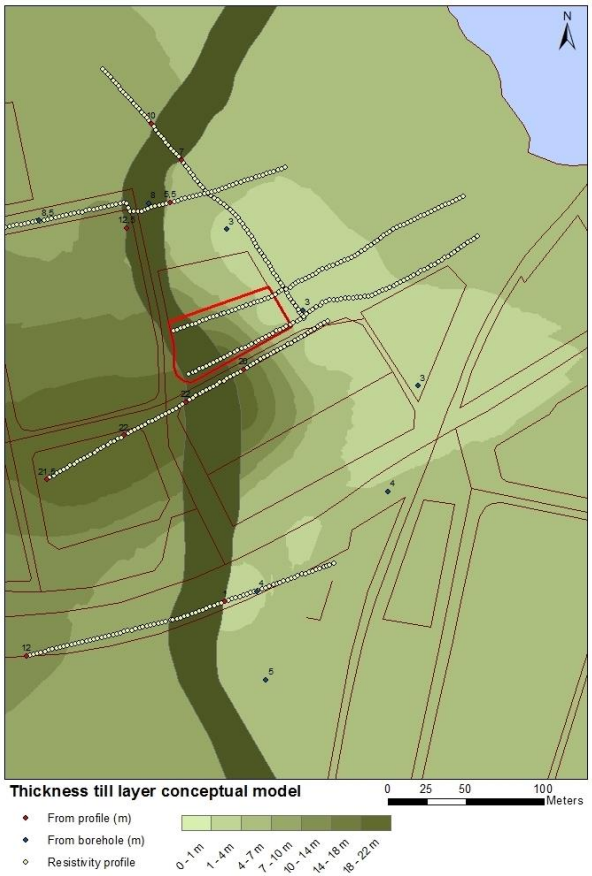

Figure 49. Horizontal overview of the thickness of the till layer in model 2 and 3. The dark blue points show the location of the boreholes and attached number the observed thickness and the red dots information about the thickness retrieved from the resistivity profiles. The red polygon shows the location of Färgaren 3

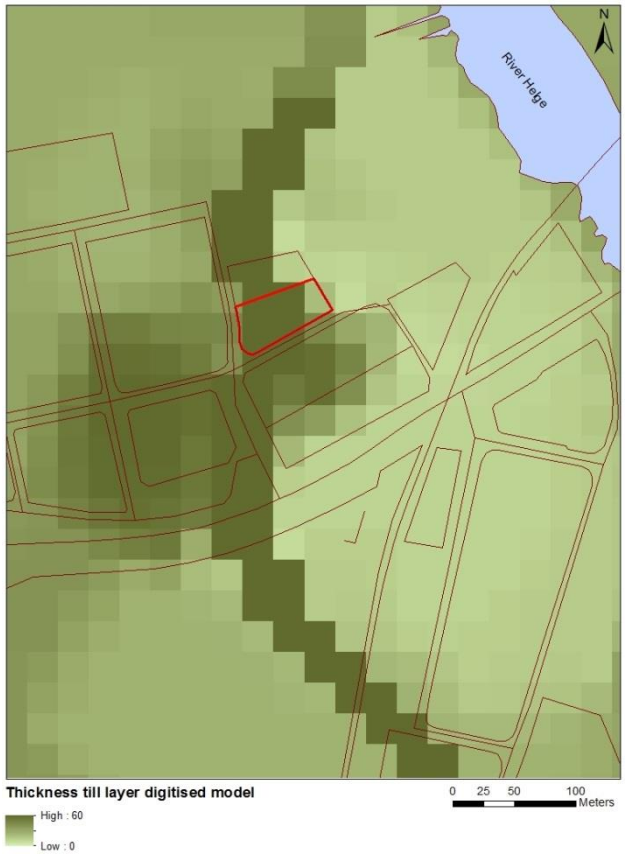

Figure 50. The digitised version of the till layer, version 2 and 3